CHALMERS

Scheduling for VGOS Twin-Telescopes

Master of Science Thesis

PAUL GNILSEN

Department of Earth and Space Sciences
Division of Space Geodesy and Geodynamics
CHALMERS UNIVERSITY OF TECHNOLOGY
Göteborg, Sweden, 2016

Technische Universität Wien
Department of Geodesy and Geoinformation
Vienna, Austria

Chalmers University of Technology
Department of Earth and Space Sciences
Gothenburg, Sweden

Master Thesis

Scheduling for VGOS Twin-Telescopes

carried out in order to obtain the academic degree
Master of Science

supervised by

Prof. Dr. Johannes Böhm
Department of Geodesy and Geoinformation, Vienna University of Technology

and

Prof. Dr. Rüdiger Haas
Department of Earth and Space Sciences, Chalmers University of Technology

co-supervised by

Dipl.-Ing. Caroline Schönberger

by

Paul Gnilsen

Matr.-No.: 0926382

Vienna/Gothenburg

Paul Gnilsen

Abstract

The technique of Very Long Baseline Interferometry (VLBI) allows the estimation of all five Earth Orientation Parameters (EOP), the International Celestial Reference Frame (ICRF) and it is a primary contributor to the International Terrestrial Reference Frame (ITRF), in particular with information about its scale. The International VLBI Service for Geodesy and Astrometry (IVS) aims at an improvement of accuracies for the next generation VLBI system by one order of magnitude, as compared to today's level. This concerns the accuracies of the station positions and velocities that should be achieved at the 1 mm and 0.1 mm/year level, respectively, within the next years. Therefore a concept has been developed which was called VLBI2010 and then VLBI Global Observing System (VGOS). To reach these ambitious aims new VLBI Twin Telescopes (TT) are built next to already existing radio telescopes. The smaller TT, which are faster in their slewing movement, shall contribute to the goals of VGOS by an increasing number of scans and observations per site at a time.

This study covers the utilisation of TT and goes into more detail about suchlike stations at the sites of Onsala in Sweden and Wettzell in Germany, which are in the works and are already built respectively. Therefore a global VLBI campaign named CONT11, which was held in September 2011, is rescheduled and simulated to compare the results between the subjoined TT and all other thirteen participating stations from this network of telescopes. As expected the distribution and absolute number of scans and observations in conjunction with these TT surpass the other antennas. Also the differences between simulated and estimated zenith delays are smaller for TT. However, baseline length repeatabilities derived from Monte Carlo simulations do not yield improved values for TT for the scheduling strategies tested in this thesis. Consequently more research for scheduling Twin Telescopes is required.

Kurzfassung

Very Long Baseline Interferometry (VLBI) ist eine Technik, die es ermöglicht alle fünf Erdorientierungsparameter (EOP) sowie das Internationale Celestial Reference Frame (ICRF) zu schätzen. Außerdem leistet sie einen Hauptbeitrag zur Bestimmung des Internationalen Terrestrial Reference Frame (ITRF), insbesondere seines Maßstabes. Der Internationale VLBI-Service für Geodäsie und Astrometrie (IVS) strebt eine Verbesserung der Genauigkeiten für die nächste Generation von VLBI-Systemen um eine Größenordnung im Vergleich zu dem heutigen Niveau an. Dies betrifft die Genauigkeiten der Stationspositionen und -geschwindigkeiten, die auf 1 mm bzw. 0.1 mm/Jahr aufgelöst werden sollen. Um diese Ziele zu erreichen wurde ein Konzept realisiert, welches als VLBI2010 und später VLBI Global Observing System (VGOS) bezeichnet wird. Dafür werden mehr und mehr VLBI Zwillingsteleskope neben bereits existierenden Stationen gebaut. Diese kleineren Teleskope sollen mit einer höheren Anzahl an Scans und Beobachtungen sowie schnelleren Drehbewegungen dazu beitragen, die Ziele von VGOS in den nächsten Jahren zu erreichen.
Diese Arbeit untersucht den Einfluss und die Verwendbarkeit von solchen Zwillingsteleskopen an den Standorten Onsala in Schweden und Wettzell in Deutschland. Die Positionen wurden deshalb gewählt, weil an diesen solche Antennen bereits existieren (Deutschland), bzw. in kürze gebaut werden (Schweden). Hierfür wird mit CONT11, eine globale VLBI Kampagne aus dem Jahr 2011, neu simuliert um die Ergebnisse zwischen den beigefügten Zwillingsteleskopen und allen anderen dreizehn teilnehmenden Stationen aus diesem Netzwerk zu vergleichen.
Wie erwartet übertreffen die absoluten Anzahlen der Scans und Beobachtungen der Zwillingsteleskope jene der anderen Antennen. Die Differenzen zwischen simulierten und geschätzten Zenitverzögerungen sind erwartungsgemäß kleiner für diese neuen Stationen. Die von Monte-Carlo-Simulationen abgeleiteten Basislinienwiederholbarkeiten ergeben jedoch keine besseren Werte in der Simulation der Kampagne. Somit ist mehr und tiefgrüdigere Forschung mit Zwillingsteleskopen erforderlich.

Acknowledgements

I would like to express my gratitude to my supervisors Professor Rüdiger Haas from the Chalmers University of Technology in Gothenburg and Professor Johannes Böhm as well as Dipl.-Ing. Caroline Schönberger from the Technische Universität Wien. For their comments, remarks, and support through the entire process of this thesis.
Furthermore I would like to thank all PhD students at the Onsala Space Observatory for their succour in acclimatising in the first weeks and who always had a friendly ear regarding coding.
Many thanks also to the VLBI Team from the Technische Universität Wien and Jing Sun for their support in respect of getting VieVS up and going since day one.
On a very personal note I would like to express my gratitude to my parents as well as my partner who contributed their shares with their never-ending encouragement through the emergence of this study. Their dedication is one of the foundations this thesis rests upon.

Paul Gnilsen, February 2016

Contents

1 Introduction **1**

1.1 History of VLBI . . . 2

1.2 Modern VLBI . . . 3

1.2.1 Aims and capabilities of VLBI . . . 3

1.2.2 Data acquisition . . . 4

1.2.3 Data analysis . . . 8

1.2.4 Geometric concept . . . 10

1.2.5 Theoretical delays . . . 13

1.2.6 Station coordinates . . . 13

1.2.7 Earth orientations . . . 14

1.2.8 Atmospheric delay modelling . . . 16

1.2.9 Least-squares adjustment . . . 18

1.3 Onsala Space Observatory . . . 19

1.4 CONT11 . . . 20

1.5 VGOS . . . 21

1.6 VieVS . . . 23

1.6.1 Scheduling strategies for VLBI Telescopes . . . 24

1.7 Twin Telescopes . . . 25

1.7.1 Observation modes for Twin Telescopes . . . 26

2 Experiments with VLBI scheduling **28**

2.1 Applied Schedules in VieVS . . . 28

2.2 Simulations . . . 29

2.2.1 Turbulence parameters . . . 30

2.3 Least Squares Adjustment . . . 31

3 Results of VLBI scheduling **32**

3.1 Number of scans and observations 32

3.2 Observation Time 34

3.3 Distribution of scans 35

3.4 Atmospheric delays 38

3.4.1 Mean standard deviation of zenith delays 42

3.5 Baseline Length Repeatability 43

4 Conclusion **48**

5 Outlook **49**

6 Acronyms **54**

1 Introduction

VLBI Global Observing System (VGOS) is a concept realised by the International Very Long Baseline Interferometry Service for Geodesy and Astrometry (IVS). It aims for an improvement of accuracies in terms of station positions and velocities to 1 mm and 0.1 mm/year, respectively. This shall be achieved by means of new types of telescopes, which carry out broadband observations and are smaller in size. More precisely, this study will treat the new Twin Telescopes (TT) and their impact on VLBI sessions.

TT are built closely beside already existing Very Long Baseline Interferometry (VLBI) telescopes, but are usually smaller in size. They have their advantages in much faster slewing and tilting time compared to the original telescopes. This new design is essential in order to conduct more observations in a shorter time. For that reason, TT should provide an improved treatment of the atmosphere's turbulences and their effects on observations which is the limiting factor of today's VLBI. These objectives can be achieved by means of their more compact architecture. It is also expected that the use of TT will assure continuous observations, so-called 24/7 observations, and the delivery of precise station coordinates.

Several projects following the VGOS concept have been initialised internationally during the last years. Some of them also include the TT approach, for example the projects in Wettzell (Germany), Ny-Ålesund (Norway), and Onsala (Sweden). With VGOS the next generation VLBI network is thus already in development and first observations can be expected within the next years.

To investigate all these emphases this thesis covers several schedules and simulations with TT. This comprises the application of several observing modes and strategies of the antennas, e.g., the number of sources observed simultaneously or the estimation interval of atmospheric delays. Therefore the Vienna VLBI Software (VieVS) was used which was developed by the Technische Universität Wien.

1.1 History of VLBI

Very Long Baseline Interferometry, or VLBI for short, is a radio wave-based space geodetic technique which was first launched in the late 1970s. Karl G. Jansky set the basis of the radio astronomy, when he first measured radio signals from cosmic sources outside our solar system already in 1933. After World War II this branch of astronomy experienced its most rapid development to explore the universe. But soon it became clear that the resolution of a single radio antenna was limited. In 1967 working groups from Canada and the United States designed and successfully launched two-station interferometers independently [Bare et al., 1967]. The principle of interferometry, which was already familiar from optics, was used to refine this method of observation. From then on the recorded signals were down-converted in terms of frequency, tagged with a time stamp and memorised on former tape bands. These bands from at least two telescopes were sent to correlation centres where the recorded signals from one source were cross-correlated and integrated. One difficulty was that the signal was very weak compared to the background noise. For improvement the signals received an amplification later on. This new technique made the need for phase-stable connections among the observing stations dispensable. Also the baseline could be increased many times over and a higher resolution could be achieved. The development of high-precision atomic clocks in the 1960s finally made it possible to realise interferometer connection along baseline lengths of several thousand kilometres without a cable.
In the following years many potential applications of geodetic VLBI were discerned. The very first experiments to achieve the highest accuracy with VLBI were performed in the United States. More precisely, it was the baseline between the Haystack Observatory (Massachusetts) and the National Radio Astronomy Observatory of Green Bank (West Virginia) with a length of about 845 km. Since these first developments the capabilities of VLBI have been expanded dramatically. For instance, the first geodetic observations were recorded with only 0.72 Mbit/s. Nowadays, VLBI systems record with at least 1024 Mbit/s. Even more important, the accuracies of station positions increased from a few metres to today's level of one centimetre or lower. This was made possible by means of wider bandwidths, two frequency observations to reduce the ionospheric disturbances, a reduction of the systems' temperatures and phase calibrations. Further improvements were achieved in observing strategies, analysis methods, and modelling of physical processes, but also the implementation of a bandwidth synthesis technique. This helped to extend

the recordable bandwidth which was as a limiting factor of tape recorders at that time. Therefore it was possible to attain group delay precisions of 1 ns which equalled a 30 cm error in radial direction.
One of the first major achievements was reached when the transatlantic baseline between Haystack and Onsala was estimated. More than 30 experiments revealed a baseline rate of 17 mm/y with a statistical standard deviation of ±2 mm/y from 1980 to 1984.
The reason why VLBI is of great importance for geodesy is because it is the only technique that provides the full set of Earth orientation parameters. Furthermore the geometric basic equation of radio interferometry comprises the direction and absolute value of the base vector between the antennas together with the position of the radio source. Out of the mostly very weak and noisy radio waves the time delay and subsequent geodetic targets can be determined with high precision. This requires an intensive collaboration with other disciplines, such as communications and electrical engineering [Schuh and Plank, 2011].

1.2 Modern VLBI

The geodetic VLBI technique measures the difference in arrival times of incoming signals from space by means of cross-correlation. Most of the time these radio signals are emitted by and travelling from quasars to Earth, but also satellite's signals have already been recorded.
Quasars, at a distance of billions of light years away from Earth, are permanently emitting electromagnetic waves in a wide range of band spectrum hitting our planet. In fact, only a small percentage of quasars emit radio waves. Most of them also include infrared, visible light, ultraviolet radiation, X rays, and some of them possibly gamma rays [Advameg, 2015]. Only a relatively tiny window within the spectrum is being used for radio interferometry by means of the telescopes, however. These signals are recorded within the S-Band (2.3 GHz) and X-Band (8.4 GHz). The resolution of an observation corresponds to the largest distance between telescopes in the VLBI network.

1.2.1 Aims and capabilities of VLBI

If VLBI observations were performed for many hours, they could be outlined as a session. Sessions run for several days, stated as a VLBI campaign. This ensures a contribution to

the attainment of several objectives. One of those is the practical realisation and ongoing retention of the International Celestial Reference Frame (ICRF), but it also concurs with the preservation of the International Terrestrial Reference Frame (ITRF) [Petrachenko et al., 2009]. Furthermore it is valuable to determine a full set of Earth Orientation Parameters. This matter of fact is indispensable for positioning and navigation on Earth and in space together with the previously described reference frames. In addition to that, VLBI delivers nutation and precession of the Earth's rotation axis to serve the exploration of the Earth's movement in space. Finally, the atmosphere's wet part in the troposphere can be estimated together with the Earth's rotation angle dUT1 (UT1 - UTC). While UT1 is the time scale derived from the Earth's rotation, the Coordinated Universal Time (UTC) is derived from the International Atomic Time (TAI) directly and only differing in seconds.

To achieve some of these goals also other techniques than VLBI can be used with different capacities. They mostly work with radio waves, but also with laser and other types of signals. Table 1.1 shows several geodetic space techniques and their areas of application.

1.2.2 Data acquisition

VLBI is an observing technique where antennas need to be controlled and oriented towards radio sources in space to generate data through its observations. Thus observation schedules are necessary. The NASA developed the package SKED at the Goddard Space Flight Center which is the common standard for generating suchlike observation plans. Certain observation strategies are also described in chapter 1.7.1. The minimum elevation angle is usually 5° to 10°, but obstacles on the local horizon of each antenna have to be considered. Apart from this, antennas use different integration times to obtain the required signal-to-noise-ratio (SNR) per baseline [Petrov et al., 2009]. The extragalactic sources emit radiation which first expand in the shape of spherical waves. On Earth telescopes record them as plane waves due to the enormous distance they travel through space. The signal first arrives at the primary paraboloidal dish, then hits the hyperboloidal subreflector and finally enters the feedhorn in the centre of the antenna. Figure 1.1 shows a detailed view of the 20 metre diameter telescope in Wettzell, Germany. First the signals receive an amplification since they come in very weakly. Next a heterodyning from radio frequencies to intermediate frequencies is done of several hundred MHz of magnitude.

Parameter	VLBI	GNSS	DORIS	SLR	LLR	Altimetry
ICRF (quasars)	X					
Nutation	X	(X)		(X)	X	
Polar motion	X	X	X	X	X	
UT1	X					
Length of day	(X)	X	X	X	X	
ITRF (stations)	X	X	X	X	X	(X)
Geocentre		X	X	X		X
Gravity field		X	X	X	(X)	X
Orbits		X	X	X	X	X
LEO orbits		X	X	X		X
Ionosphere	X	X	X			X
Troposphere	X	X	X			X
Time/frequency	(X)	X		(X)		

Table 1.1: Geodetic space techniques and their capabilities. The following abbreviations are applied: GNSS (Global Navigation Satellite Systems), DORIS (Doppler Orbitography and Radiopositioning Integrated by Satellite), SLR (Satellite Laser Ranging) and LLR (Lunar Laser Ranging). Modified from [Schuh and Behrend, 2012].

This is followed by a down-conversion to baseband frequencies which is done in multiple frequency sub-bands or channels simultaneously. There the signals are band-limited to a few MHz and also digitised and sampled [Sovers et al., 1998]. During the whole process the system temperature for S- and X-band constantly remains between 20 and 100 Kelvin. Lastly the recorded data is stored on magnetic disks and shipped to the correlation centres. In recent time however, technological advancements also allowed recorded data from short term sessions to be forwarded to the correlation centres in real-time via high-speed broadband communication links (e-VLBI).

In general VLBI radio telescopes need large collecting areas as well as high sampling and recording rates because the signal flux density is small. It is in the order of 1 Jan-

Figure 1.1: The paraboloidal reflector with the subreflector and the feedhorn of the 20 metre diameter telescope in Wettzell, Germany [Heinkelmann, 2013].

sky ($1\ Jy = 10^{-26} W m^{-2} Hz^{-1}$) or lower [Association, 2011]. Jansky is the unit for the spectral flux density. It represents the arriving energy per time, per area and per frequency interval. Due to the far distance to the quasars the magnitude is very small. For example the strongest known radio sources have a flux density in the order of 1 - 100 Jy. Nevertheless telescopes need to have compact architectures and to be equipped with powerful engines to ensure fast slewing movements.

During the whole data processing phase shifts may occur in the recorded signals caused by the instrumentation which have to be calibrated in order to take full advantage of precise hydrogen (H) masers. The calibration is done by generating a signal of a known phase and by feeding it into the recorded signal [Rogers, 1975]. After this calibration wave has passed the whole instrumentation it is investigated and possible phase shifts can be revealed. This is of importance since phase shifts can interfere the estimated phase and the group delay, if not taken into account. Other influences such as Doppler shifts caused by the Earth rotation or potential hardware delays, e.g. length variations of cables, also have to be corrected.

When the recorded signals are merged, an interference pattern arises. This is done in certain correlator centres, such as the Max Planck Institute for Radio Astronomy in Bonn, Germany and the Haystack Observatory in Westford, U.S.A. or the National Institute of

Information and Communications Technology in Kashima, Japan. Basically a correlator determines the differences in arrival times of the incoming signal at the antennas by comparing the recorded bit streams. The correlation function is described in equation 1.1. $V_1(t)$ and $V_2(t)$ represent the antenna voltages where the latter stands for the complex conjugate, denoted with the asterisk. T is the averaging interval. The group delay τ of the signal is determined by finding the maximum of R through the cross-correlation [Sovers et al., 1998].

$$R(\tau) \;=\; \frac{1}{T} \int_0^T V_1(t) \;\cdot\; V_2^*(t-\tau) \;\cdot\; dt \tag{1.1}$$

In the course of the correlation the amplitudes and phases will be determined every one to two seconds in parallel for usually 14 frequency channels ω_i (see table 1.2). A post-

X-Band [MHz]	S-Band [MHz]
8182.99	2212.99
8222.99	2222.99
8422.99	2257.99
8562.99	2297.99
8682.99	2317.99
8782.99	2322.99
8842.99	
8862.99	

Table 1.2: 14 frequency channels in which amplitudes and phases are determined in parallel every one to two seconds.

correlation software fits the phase Φ_0, the group delay τ_{gd}, and the phase rate τ'_{pr} to the samples $\Phi(\omega_i, t_j)$ from these frequency channels ω_i at the times t_j. From the measured phases $\Phi(\omega, t)$ observables can be derived via a bilinear least-squares method (see equation 1.2).

$$\Phi(\omega, t) \;=\; \Phi_0(\omega_0, t_0) + \frac{d\Phi}{d\omega}(\omega - \omega_0) + \frac{d\Phi}{dt}(t - t_0) \tag{1.2}$$

where

$$\tau_{gd} = \frac{d\Phi}{d\omega}, \quad \tau'_{pr} = \frac{1}{\omega_0}\frac{d\Phi}{dt}, \quad \tau_{pr} = \frac{\Phi_0}{\omega_0} \tag{1.3}$$

and the phase rate τ'_{pr} is used to fix group delay ambiguities. Further what is really essential is the group delay τ_{gd}, which is the main geodetic VLBI observable. Its resolution can be achieved with the SNR and the RMS spanned bandwidth B which equals a RMS of the

frequency over its mean:

$$\sigma_\tau = \frac{1}{2\pi} \frac{1}{SNR \cdot B} \tag{1.4}$$

where an increase of B will reduce σ_τ for about the same factor. The SNR is formed by:

$$SNR = \eta \cdot \rho_0 \cdot \sqrt{2 \cdot B_r \cdot T} \tag{1.5}$$

where η represents a digital loss factor of the system, ρ_0 is the correlation amplitude, depending on both noise temperatures of the antenna and the source, B_r is the recorded bandwidth while T is a coherent integration time in the correlation process [Takahashi et al., 2000].

Nowadays baselines can be determined very accurately, but only within a certain length. VGOS aims for related accuracies for longer baselines which, however, are still non-pareil due to phase ambiguities.

1.2.3 Data analysis

The subsequent data analysis aims for an exact delineation of the signals at the time of observation followed by a least-squares estimation which allows certain parameters to be determined (see chapter 1.2.9). To reach highest precision in the final output the raw observations have to be corrected for systematic effects which are without a doubt limiting factors. Figure 1.2 shows a flow diagram of VLBI data analysis.

Basically the whole process can be differenced into two streams, one of which represents the true VLBI observables, whereas the other stands for the theoretical and computed delay, derived from known station and source coordinates as initial values. The observed delay τ receives adaptations in terms of instrumental calibration and environmental corrections, e.g. for cancelling out the ionospheric delays. Whereas $\tau_{computed}$ can be built from Earth models about its deformation, known Earth orientation parameters and relativistic delay models. In terms of the troposphere, fast slewing antennas are required to observe through steady layers. With these two delays the observed-minus-computed delay will be calculated in the parameter estimation algorithm, where then a least-squares adjustment is applied. Possible group delay ambiguities result from observations from the multichannel frequency setup (see table 1.2 on page 7). They cover the full bandwidth of the observation frequencies in S-band (2.3 GHz) and X-band (8.4 GHz). The shift level of the residuals and therefore

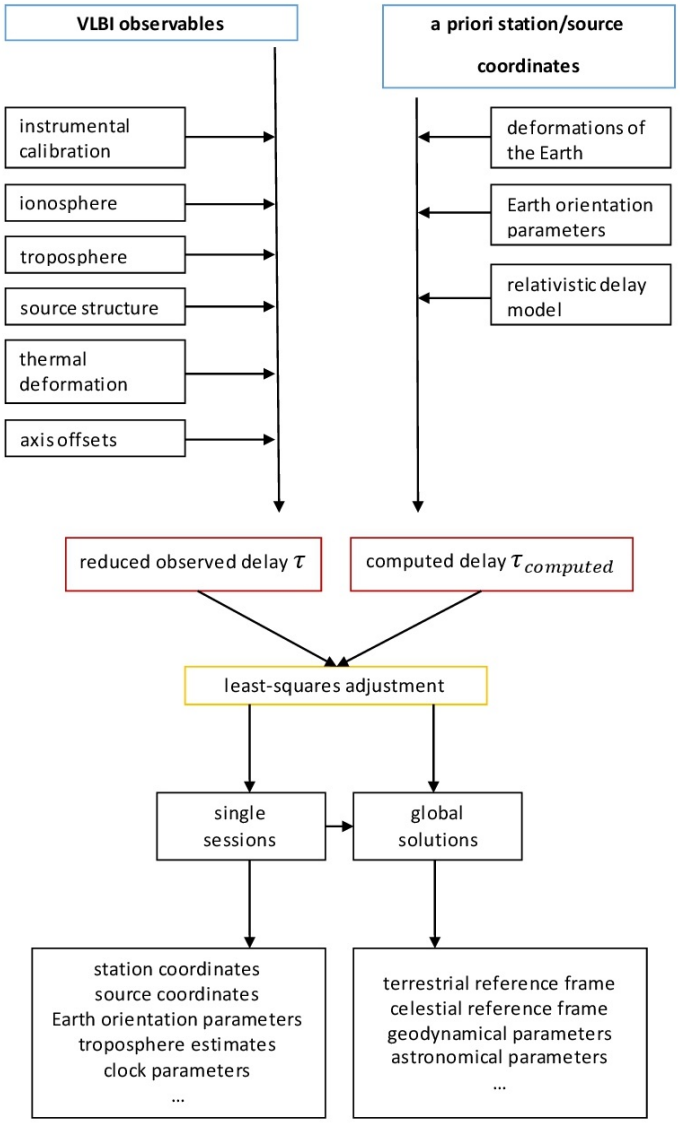

Figure 1.2: Flow diagram of geodetic VLBI analysis and its capabilities. Modified from [Schuh].

the group delay observables can be selected by means of the group delay rates τ'_{pr} [Schuh and Böhm, 2013]. Since the ionosphere is a dispersive medium, two frequency observations combined with linear combination can reduce this environmental delay:

$$\Delta\tau_X^{ion} = (\tau_X - \tau_S) \cdot f_S^2/(f_X^2 - f_S^2) \tag{1.6}$$

which means that the group delay corrections in X-band can be derived from differences in group delay measurements in both bands. Here appears a disparity to the GPS System where frequencies are closer together. This means that the factor to transform this difference into an adaptation for higher bands is even smaller.

1.2.4 Geometric concept

As a matter of fact, VLBI can only be carried out with at least two telescopes on Earth, which means that one telescope is recording the same signal earlier than the other. For the sake of clarity vectors are written in bold characters henceforth. The first arrival time t_1 is kept as a reference for the VLBI analysis (fig. 1.3). The baseline vector $\mathbf{B}$, which is spanned between the two stations, can be reduced to a rectangular projected baseline $\mathbf{U}$. This stands in direct relation to the direction to the radio source $\boldsymbol{s_0}$. With the reception time t_2 of the signal at the second station the observed delay can be described as $\tau = t_2 - t_1$. Together with the speed of light c this delay can be expressed in terms of a vector $\boldsymbol{s_0}$ and the distance $\mathbf{B}$ (equation 1.7 and 1.8).

$$\tau = t_2 - t_1 = -\frac{\boldsymbol{B} \cdot \boldsymbol{s_0}}{c} \tag{1.7}$$

$$L = \mathbf{B} \cdot cos(\beta) = c \cdot \tau \tag{1.8}$$

Repeated determinations of τ via several radio sources observed in rapid sessions deliver an over-determined baseline vector $\mathbf{B}$. The signal delay τ is time-dependent, which means it varies. The reason is that the interferometers move altogether with the Earth through space with respect to the celestial reference frame where also quasars are defined. Observations are made in low GHz frequency range and the signals are recorded with a time stamp

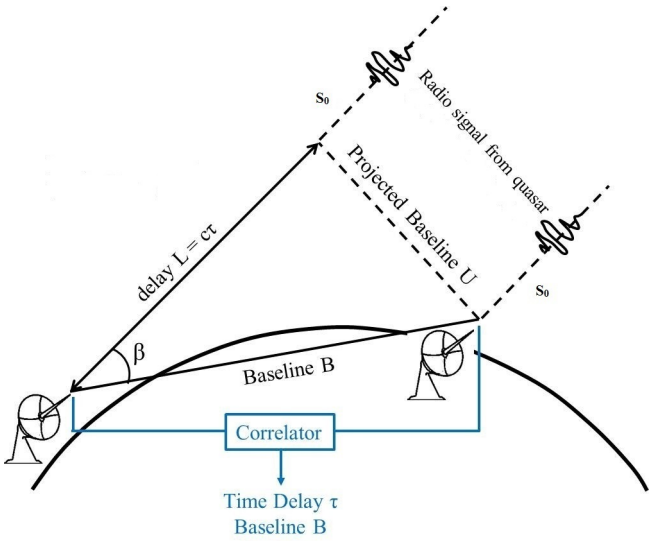

Figure 1.3: The geometric concept of Very Long Baseline Interferometry. Vectors are displayed in bold type. Modified from [Computational Physics, 2014]

for the subsequent correlation. Therefore it has always been a primary target to involve more precise and long term stable clocks such as hydrogen (H) masers. One of these H-maser's characteristics is that they reach their highest accuracy with 10^{-14} Allan standard deviation (ASD) at 50 minutes after the beginning of the recordings. All participating stations are connected for data interchange to allow the correlation in time. To make this happen, all stations follow the UTC time format.

In the course of the following correlation, which is described in chapter 1.2.2, certain corrections, necessary for high accuracy positioning, need to be applied. For instance an additional path length at the second antenna. The radio wave has to travel further until it hits it. Besides the Earth rotation requires corrections that need to be applied. Or the relative delay, which is determined through the peak of the cross-correlation, delivers also a value for τ [Schuh and Behrend, 2012]. In addition to the geometrical delay, previously designated as τ, other significant terms can be added, which together make up the total delay:

$$\tau = \tau_g + \tau_{ab} + \tau_{clk} + \tau_{trop} + \tau_{ion} + \tau_{rel} + \tau_{inst} \tag{1.9}$$

where

- τ_g is the geometric delay;
- τ_{ab} represents daily aberrations;
- τ_{clk} describes errors in clock synchronisations of the observatories;
- τ_{trop} is a contribution of the Earth's lowest layer of the atmosphere;
- τ_{ion} is a contribution of the free electron content in the Earth's atmosphere;
- τ_{rel} is a relativistic correction;
- τ_{inst} is a hardware delay caused by instrumentation.

The individual terms all have a more or less great influence on τ. To guarantee a proper separation of these terms, observations under many elevation angles are required [Pany et al., 2010]. Further they must be removed in the post-processing of a VLBI campaign. This is done mostly through calibration, two frequency observations (elimination of the ionospheric delay) or by calculation and modelling with the help of local measurements (for the troposphere).

From τ and $\mathbf{B}$ their baseline length repeatabilities can be derived which are a measure of station coordinate accuracies, together with other astronomical and geodetic parameters. One particular output of VLBI is the angle β spanned by the baseline $\mathbf{B}$ and the delay $\boldsymbol{s_0}$ (fig. 1.3). It can be obtained under very high accuracy during a VLBI session. This is very essential for deriving Earth orientation parameters since even the merest change of $\mathbf{B}$ and β can be detected [Schuh and Behrend, 2012]. If there are many telescopes forming a VLBI session over several hours or even days, there are also many scans and observations carried out by these telescopes. As an explanation observations of quasars are single scans of telescopes taken together. Further the time delay can be computed out of known station and source coordinates in advance $\tau_{computed}$. When forming the difference $\tau - \tau_{computed}$ and subsequent adjustment, residuals for the baselines and both station and source coordinates can be derived [Schuh and Plank, 2011].

1.2.5 Theoretical delays

In the course of the least-squares adjustment over the observed-minus-computed delays various models are applied, such as the determination of the station coordinates in its observed epoch with the following rotation from the terrestrial frame to the celestial frame. There the baselines are calculated out of the computed delays. Furthermore corrections are applied, as described already. These corrections and further conventions are defined by the International Earth Rotation and Reference Systems Service. Additional IVS convention concern the thermal expansion of telescopes, when actively observing [Schuh and Böhm, 2013].

1.2.6 Station coordinates

First coordinates and velocities of the stations are calculated for the time of observation. These values are mean values given in a realised International Terrestrial Reference System (ITRS), like the ITRF2008 or more particular VLBI frames like the VTRF2008 [Böckmann et al., 2010]. To add a relation of time reference epochs are taken, like J2000.0 which is the 1st of January at 12 pm in Terrestrial Time. All of these frames are related to this time and tide-free systems.
In the further course station coordinates are corrected by several models. These models include deformations of the Earth crust in periodic and aperiodic ways, like for the solid Earth tides which are the largest periodic corrections, but also ocean and pole tide loading. The solid Earth tides reach deformation magnitudes of ± 20 cm vertically and around ± 6 cm in horizontal direction in diurnal and semi-diurnal periodicity. Other possible displacements can reach up to ± 10 cm in coastal areas and even on smaller islands, caused by water masses [Scherneck, 1991]. Ocean tides and loading are way more difficult to handle due to irregular shorelines and landforms. Furthermore the atmosphere's thermal heating engenders pressure tides on Earth which arise every 12 and 24 hours. All these influences need to be taken into account at the actual observation level in order to meet the demands of high precision VLBI. Nevertheless especially aperiodic deformations, caused by the non-tidal atmosphere, ocean, and hydrological loading, can affect VLBI calculations sensitively, there is no general agreement or any international convention whether these factors should be corrected or not. On the one hand atmosphere loading is intercepted by no-net-rotation

(NNR) and no-net-translation (NNT) conditions to some degree, if neglected. Therefore it does not make its presence felt in estimated coordinate time series too much. Moreover applying these corrections in data analysis later on is not always very useful since non-tidal atmospheric loading varies significantly within a day. The variation would still not be considered. On the other hand scientists argue that there are no consistent models available to correct the non-tidal atmosphere loading at observation level [Petrov and Boy, 2004]. Furthermore the existing models lack in accuracy and the entire exclusion of all models would expose the direct loading signals via coordinate time series in which geophysicists are interested.

1.2.7 Earth orientations

Right after station coordinates are determined they need to be transformed from the ITRS into the Geocentric Celestial Reference System (GCRS). The transformation at the time t is denoted as:

$$[GCRS] = Q(t) \cdot R(t) \cdot W(t) \cdot [ITRS] \tag{1.10}$$

where the transformation matrices $Q(t)$, $R(t)$, and $W(t)$ are related to the celestial pole movement given in the GCRS, to the rotation of the Earth around the pole axis, and to the movement of the Earth's pole respectively [Petit and Luzum, 2010]. $R(t)$ comprises the Earth rotation matrix with the Earth rotation angle θ between the Terrestrial Intermediate Origin (TIO) and the Celestial Intermediate Origin (CIO). UT1 which is determined from θ and can only be determined by VLBI according to fable 1.1, is defined by international conventions as the following:

$$\theta(T_u) = 2\pi \cdot (0.7790572732640 \ + \ 1.00273781191135448 \cdot T_u) \tag{1.11}$$

where Tu = (Julian UT1 date − 2451545.0) and UT1 = UTC + (UT1-UTC) = UTC + dUT1. dUT1 is the difference between the Universal Time (UT1) and Universal Time Coordinated (UTC) and can only be observed by VLBI. UTC is connected to the International Atomic Time (TAI) by adding leap seconds at irregular intervals to compensate for fluctuations in Earth rotation, mainly its slowing. The atomic clocks, which produce weighted means of signals, have their sites all over the world. These leap seconds keep UTC within 0.9 seconds of universal time, UT1 [Schuh, 2011]. Furthermore the length of

day can be observed via satellite techniques, such as GNSS and SLR, since they are based on UT1 with one of their Keplerian elements, the right ascension of the ascending node of the satellite orbit. The former is derived from the negative derivation of UT1-UTC.
The matrix $W(t)$ consists of the polar motion with its coordinates x_p and y_p, of the Celestial Intermediate Pole (CIP) in an Earth-fixed frame, and of a correction angle s'. The latter positions TIO origin on the equator of the CIP. TIO (terrestrial) and CIO (celestial) set the reference meridians in their respective systems.
Finally the matrix Q(t) comprises rotations around the coordinate axes of the CIP, given in the celestial frame and the correction angle s' again. The CIP is of great importance for space geodesy, since it is the reference pole of measurements with its observation axes. Basically the CIP is a theoretical construct which is never coextensive with other physical axes like the rotation axis. However, the motion of the ITRS pole w.r.t the GCRS can be separated into a terrestrial part and a celestial part with the CIP. The latter consists of the precession and nutation of the Earth's rotation axis and of all periodic motions with oscillations longer than two days. The terrestrial part (polar motion, x_p and y_p) comprises motions outside of 0.5 cycles per siderial day in the ITRS. Only frequencies outside of the [0.5 , 1.5] interval per siderial day are represented in the ITRS.
One part of the CIP motion can be dealt with a conventional precession/nutation model. If such a model does not take all CIP parts into account, VLBI can observe them or they can be requested as pole offsets from the International Earth Rotation and Reference Systems Service (IERS). Celestial pole offsets are errors of the precession-nutation model partly caused by Free Core Nutation (FCN). This FCN is a phenomenon, stemming from the non-alignment between the rotations axes of both the Earth's mantle and its core [Dehant and Mathews, 2009]. The period of this retrograde movement in the GCRS is roughly 430 days and appears with around 10 mm on the Earth's surface. A forecast is impossible to apply here, but it cannot be excluded totally in case of high positioning accuracy demands. Therefore space geodetic observations deal with precession, nutation, polar motion, and dUT1, since they cannot be modelled sufficiently. The IERS provides parameter estimations. If no parameter estimations are conducted, pole coordinates (x_p, y_p) can be calculated as the following [Englich et al., 2008]

$$(x_p, y_p) = (x, y)_{IERS} + (\delta x, \delta y)_{ocean} + (\delta x, \delta y)_{libration} \tag{1.12}$$

where $(x, y)_{IERS}$ are pole coordinates provided by the IERS. $(\delta x, \delta y)_{ocean}$ represent ocean tides which can also lead to diurnal and semi-diurnal variations of the CIP. $(\delta x, \delta y)_{libration}$ stands for forced variations of the pole coordinates. They emerge less than every two days in space. The IERS provides Lagrange interpolated $(x, y)_{IERS}$ pole coordinates however, they cannot be applied to polar motion rate estimations to be used for Earth rotation since it is not a linear interpolation. The effects of ocean tides and libration are similarly difficult to calculate. Tidal terms can be abstracted, prior a Lagrange interpolation of IERS parameters and attached later on. This approach effects only the Earth's rotation angle θ.

1.2.8 Atmospheric delay modelling

For very precise modelling of the atmosphere's delays on signals it is indispensable to get a link between these delays and the elevations under which the observations were carried out. This is done with so-called mapping functions (MF). These functions allow to determine the atmosphere's delays in zenith direction by simply dividing the observed slant delays by them. The resulting Zenith Wet Delays (ZWD) serve as reference values between various VieVS simulations and their observing modes in terms of atmospheric turbulences. Mapping functions are also used to estimate residual zenith delays via partial derivatives. When geodetic VLBI observations are conducted, ZD are estimated together with station heights and their clocks. The partial derivatives for ZD (i.e. the MF) are not known with arbitrary accuracy, while the partials for clocks (= 1) and station heights (= $sin(e)$) are exactly known. Since there is a correlation between ZD, station heights, and clocks, inaccuracies of the MF lead directly to errors in the last two parameters. Therefore it is tried to diminish these correlations by adding low elevation observations (5° or less) in the VLBI analysis, including the risk of further great errors. 7°−observations emerged to be sufficient to reduce correlations and enhancements of MF errors at the same time [MacMillan and Ma, 1994], [Teke et al., 2008]. Furthermore down-weighting of low elevations is an appropriate means for the adjustment [Petrachenko et al., 2009]. Future observations with fast slewing antennas enable to increase the cut-off elevation angle in order to reduce the impact of errors in the MF.

MF also allow the ZD to be estimated in a least-squares adjustment which is described later on. The atmospheric layer with the greatest importance for signal delays is the

troposphere. The troposphere can also be partitioned into a hydrostatic mf_h and a wet mf_w part. Each part is projected into zenith direction with an adapted mapping function (equation 1.13):

$$\Delta L(e) = \Delta\ L_h^z \cdot mf_h(e) + \Delta\ L_w^z \cdot mf_w(e) \tag{1.13}$$

where $\Delta\ L_h^z$ and $\Delta\ L_w^z$ are the delays of the troposphere's hydrostatic and wet part, respectively, in direction towards the zenith. $mf_h(e)$ and $mf_w(e)$ are the MF for the hydrostatic and wet part of the troposphere respectively [Böhm, 2012].

The entire layer reaches heights of up to 20 km above the Earth's surface and is responsible for the weather as it happens day by day around the globe. Furthermore it affects the signals by bending its path. This must also be taken into account when modelling the atmosphere. Other atmospheric layers are not taken into account for the simulations in VieVS.

The MF which is being used in VieVS for both the hydrostatic and the wet delay is one variant of the Vienna Mapping Function. This variant is named $VM1$ and it uses continued fraction form (equation 1.14, [Herring, 1992]):

$$mf(e) = \frac{1 + \frac{a}{1+\frac{b}{1+c}}}{sin(e) + \frac{a}{sin(e)+\frac{b}{sin(e)+c}}} \tag{1.14}$$

where e is the vacuum observation elevation. b and c are coefficients obtained from analytical functions which depend on the day of the year and the station's latitude. a accounts for both hydrostatic and wet parts and is provided as time series with 6-hour time resolution for VLBI station sites, but also on a grid with 2.0° in latitude and 2.5° in longitude resolution [Schuh and Böhm, 2013]. These coefficients come from a forecast of the European Centre for Medium-Range Weather Forecasts (ECMWF). The ZD for the hydrostatic part in equation 1.13 are derived from local atmospheric pressure measurements in high accuracy.

Applying a precise MF in VLBI is of great importance, since estimations of station heights are strongly influenced by them. If one MF is too large, the adjusted ZD is too small. This is because the observed tropospheric delay $\Delta L(e)$ remains the same. The resulting error causes greater station heights. As a rule of thumb one can say that station height errors are about one fifth of the delay errors regarding the lowest elevation angle included in the analysis. A decrease of the ZD is roughly half of the station's height increase.

For the sake of completeness it should be mentioned that the ionosphere which lies on top of the troposphere, also has a measurable influence on radio signals. It can be reduced via two frequency observations, however.

Direct ray-tracing which is the derivation of slant delays for single observations out of numerical weather models is a technique which receives much attention these days. It can lead to better baseline length repeatabilities, but also an improvement in the estimation of UT1 via intensive sessions on the Wettzell-Tsukuba baseline together with ray-traced delays at the Tsukuba station [Hobiger et al., 2008].

1.2.9 Least-squares adjustment

The observed-minus-computed delay is determined between the reduced delay τ and the computed delay $\tau_{computed}$ via parameter estimation. This can be seen at the intersection of the two branches in the flowchart of figure 1.2 on page 9. Therefore Kalman filtering can be used as well as collocation [Herring et al., 1990]. In VLBI the Gauß-Markov model gets the nod over the previous two, however, while all three of them base on the least-squares method. With the least-squares method (LSM) unknown parameters can be estimated via an overdetermined system of equations. The more telescopes there are, the more equations and observations. First and foremost the latter are greater than the unknown parameters in number. In the course of the adjustment the squared sum of weighted residuals v is minimised, since the results won't be exact for every equation. Residual errors will therefore be divided on the observations equally. LSM provides a unique solution dx of the unknown parameters.

The functional and stochastic models are a set of linearised observation equations:

$$A \cdot dx = l + v = \begin{bmatrix} A_{ro} \\ A_{po} \end{bmatrix} \cdot dx = \begin{bmatrix} l_{ro} \\ l_{po} \end{bmatrix} + \begin{bmatrix} v_{ro} \\ v_{po} \end{bmatrix} \tag{1.15}$$

$$P = \begin{bmatrix} P_{ro} & 0 \\ 0 & P_{po} \end{bmatrix} \tag{1.16}$$

where A is the design matrix consisting of A_{ro}, composed of the first derivatives of the functional model w.r.t. the estimated parameters, and of A_{po}. Since observations aren't

performed in regular intervals it may happen that no observation falls into an estimation interval of zenith wet delays. For instance the latter can be only 20 minutes long. If this happens singularities can arise in the adjustment process which make the model insolvable. Therefore a pseudo-observation matrix A_{po} is part of the matrix A which constrains the parameter's value of variability either by setting the absolute values to zero - for troposphere gradients - or by limiting the variation of the continuous piecewise linear functions. l_{ro} consists of the observed-minus-computed time delays τ and are real observations, whereas the l_{po} vector contains pseudo-observations, which is usually a zero vector. The P matrix comprises the weighting of all observation [Schuh and Böhm, 2013].
During the adjustment several parameters are estimated. This can be clock frequency offsets or troposphere gradient parameters which are not of great interest. Other clock parameters, like clock frequency drifts, can be estimated as linear or quadratic polynomials every day additionally. Moreover the estimation includes continuous piecewise linear functions with certain time segments which are estimated w.r.t. a high precision reference clock, such as H-masers in Wettzell, or Onsala. These reference clocks are set to zero for getting on to clock instabilities. Clock constraints, such as the relative variation of the piecewise linear clock function are typically chosen with 0.5 ps^2/s. Clocks themselves can be estimated every 60 minutes, which would mean a variance of 1800 ps^2 and equal a difference of $\pm$ 13 mm between two contiguous clock offsets. One problem can be clock breaks in the clocks at the stations. These have to be detected and taken into account via the quadratic polynomials which match their progression best in the VLBI session analysis.

1.3 Onsala Space Observatory

This study has been accrued at the Onsala Space Observatory (OSO) in Sweden to a large extent, where also the simulations were performed. The OSO is located around 40 km south of Gothenburg on the west coast of Sweden. It is run by the Chalmers University of Technology in Gothenburg and its related Department of Earth and Space Sciences. For this thesis the OSO has been selected for the reason of their TT which will be erected in the near future. Figure 1.4 reveals an overview of the area of the OSO and the location of its planned TT. Besides the station in Onsala several projects following the VGOS concept have been initialised internationally during the last years. Some of them also include the TT approach, for example the projects in Wettzell (Germany) and in Ny-Ålesund (Norway)

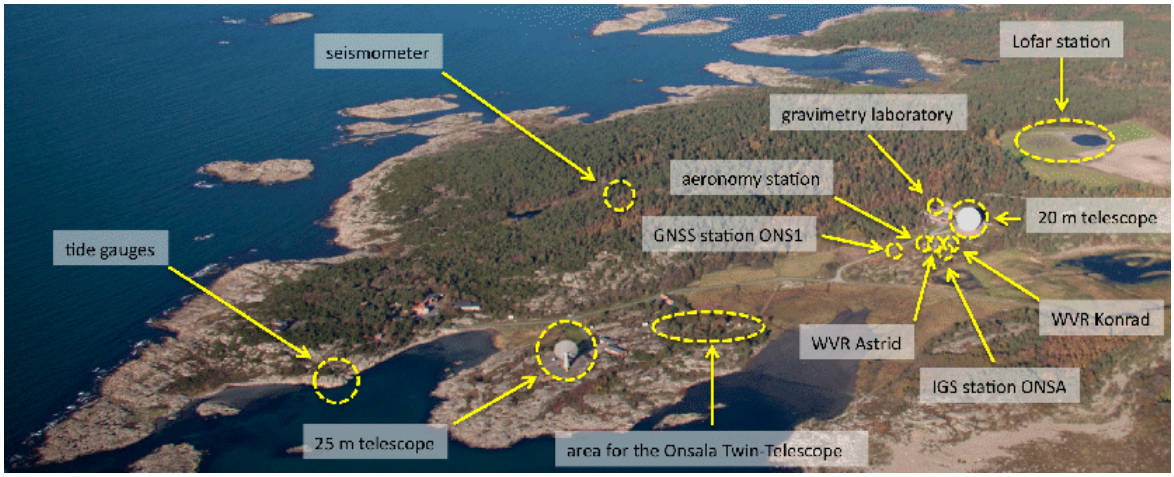

Figure 1.4: Air view of the Onsala Space Observatory near Gothenburg, Sweden. [Haas et al., 2012].

where such TT already exist or are in the process of planning. The ones in Wettzell are also involved in the course of this study. The advantages of TT are realised due to their advantageous construction design which allows to tilt and turn these telescopes faster and therefore perform more observations in a shorter time than the already existing telescopes. TT also assure continuous observations of radio sources, so called 24/7 observations to make final results available with low latency and high temporal resolution. Moreover, because there are two of them, VLBI telescopes are also able to observe radio sources by means of certain observation modes. This study will investigate some of these observation modes for TT and tries to show which one performs best in the final campaign evaluation.

1.4 CONT11

Basically all the schedules and simulations constituted on the setup of the CONT11 campaign. CONT11 was a continuation of VLBI campaigns which were first carried out in 1994. Its purpose was to investigate the Earth's reference frames, site motions of telescopes, simulations of the Earth's atmosphere and to determine Earth rotation parameters in high resolution. In September 2011 the CONT11 campaign observed quasars in space continuously between Thursday, 15^{th} 00:00:00 UT through Thursday, 29^{th} 23:59:59 UT [Rieck et al., 2012]. This means that no less than these thirteen IVS (International VLBI Service for Geodesy and Astronomy) stations took part in the simulations with two twin

telescopes at different sites additionally. Nine of them are located in the northern hemisphere and four in the southern hemisphere. The distribution of the stations can be seen in figure 1.5. As it can be see the geographical distribution of the antennas has a tendency

Figure 1.5: Distribution of the 13 participating IVS stations in the CONT11 campaign. WARK12M in Warkworth, NZL had to cancel its participation due to technical problems. [Rieck et al., 2012]

for the northern hemisphere. This is because about two thirds of the Earth's land mass are located north of the equator, but also countries are more wealthy there. For a better balance more network stations are about to be erected in Africa, South America or in the region of Australia. This is to enhance the number of telescopes used for geodetic VLBI around the world from around 30 to even more stations. The more stations there are, the more observations can be conducted. Enhancing the observation scheduling of radio sources is also a primary aim of VLBI campaigns for the future. In VLBI sources shall be observed very effectively. This means observing sources for as briefly as possible until the SNR is high enough and slewing to the next source. In the past few years VLBI observations were available for roughly 50% of the time. This percentage will be increased with the construction of new antennas.

Further aims and developments, together with requirements for geodetic VLBI systems, are defined by VGOS.

1.5 VGOS

Since progress in the field of VLBI will not remain at the status quo, there are goals for the future to make VLBI durable and more accurate. Which goals there are and how they can

be achieved is determined by VGOS. VGOS is a so-called vision created by Working Group 3 (WG3), which is subordinated to the IVS. Thus it creates current and future requirements for geodetic VLBI systems. Its main objectives are [Petrachenko et al., 2009]:

- 1 mm position accuracy and 0.1 mm/yr in velocity on global scales
- continuous measurements for uninterrupted time series of station positions and EOP
- abbreviate time of obtaining initial geodetic results to less than 24 hours

The aim of shortening the process time between observations and the first results will be achieved with faster connections of the antennas with the correlation centres via e-VLBI. The electronic transmission of data will cut down the processing time and contribute to achieve more automated station operations. This advancement is also a step away from the pre-existent magnetic tapes and hard drives which needed to be shipped for several days. Henceforth it will become possible to link radio telescopes in close to real-time. A further increase is related to the bandwidth of the signal's frequency range. With VGOS the recordings comprise frequencies from 2 GHz to 14 GHz in multiple bands [Petrachenko et al., 2009]. This high-rate sampling data acquisition shall also be enhanced to more than 8 GB/s. In addition to that, two more frequency bands will be added, which makes a total of four bands in the future, and thus more signals can be recorded and processed at the same time.

Not only will the processing components be changed, but also the architectures of the antennas themselves. Table 1.3 shows their main modifications. Their sizes shall be reduced

	Current	**VGOS**
slew speed	$\sim$ 3 deg/sec	$\geqslant$ 6 deg/sec
antenna size	5 -100 m dish	$\sim$ 12 m dish
sensitivity	200 - 15000 SEFD	$\leqslant$ 2500 SEFD

Table 1.3: Specifications of new VGOS antennas. The main alternations concern both a reduction of the slew speed and the size. Further the sensitivity should be increased. $SEFD$ stands for System Equivalent Flux Density [Petrachenko et al., 2009].

in order to increase slew speed. The aim is to accelerate the telescopes' turnarounds to more than 360 degrees per minute in azimuth. This new 12 metre reflector class will therefore affect the number of scans and observations performed during a day. As it can

be seen in later chapters a higher number of scans positively influences the modelling of the Earth's atmosphere. These investigations are based on atmospheric delays. For even better modelling of the atmosphere the delay precision shall be reduced from maximum 30 ps to 4 ps or less.
All in all, the IVS envisages a new VLBI system to enhance its technique in terms of hardware, software, and operational procedures.

1.6 VieVS

In order to achieve the aims and assess the results of VLBI analyses on which this study is based, the Vienna VLBI Software (VieVS) was used. It allows the user to estimate station positions and velocities together with their clock parameters, modelling the Earth's atmosphere and derive EOP among other things. VieVS was invented and created at the former Institute of Geodesy and Geophysics at the Technische Universität Wien starting in 2008. Basically, it is not a standalone software programme, but an application run in *Matlab*. This leads to a straightforward way to edit and adapt code fragments for someone's needs, e.g. adding new telescopes and their attributes to the antenna catalogue. For this study version 2.2 of VieVS was used. In the meantime version 2.3 was already released.
When a VLBI session is simulated it must be scheduled in advance and adjusted subsequently. VieVS uses several packages for these steps, and the first one is VIE_SCHED. This package calculates the constellation between quasars in space and the station positions on Earth for as long as the scheduling is set. Further catalogue system files must be taken into account, which include for example antenna specifications. These files are also of great importance for the selection of sources, stations and applied observing modes in the scheduling programme [Madzak et al., 2013]. In the VieVS GUI the stations also must be chosen from a worldwide catalogue including TT. Figure 1.6 shows a related screenshot including possible parameters that can be set. When VIE_SCHED is completed NGS files are created which are needed for the following simulation under VIE_SIM. This package calculates group delay observables including the three most important stochastic error sources in VLBI: wet troposphere delay, station clock, and white noise. Since the first one is of greatest magnitude, mapping functions are also taken into account in the simulation package. To simulate the atmosphere site dependent turbulence parameters must also be read in. Once again NGS files are outputted, flowing in into the last step: VIE_LSM.

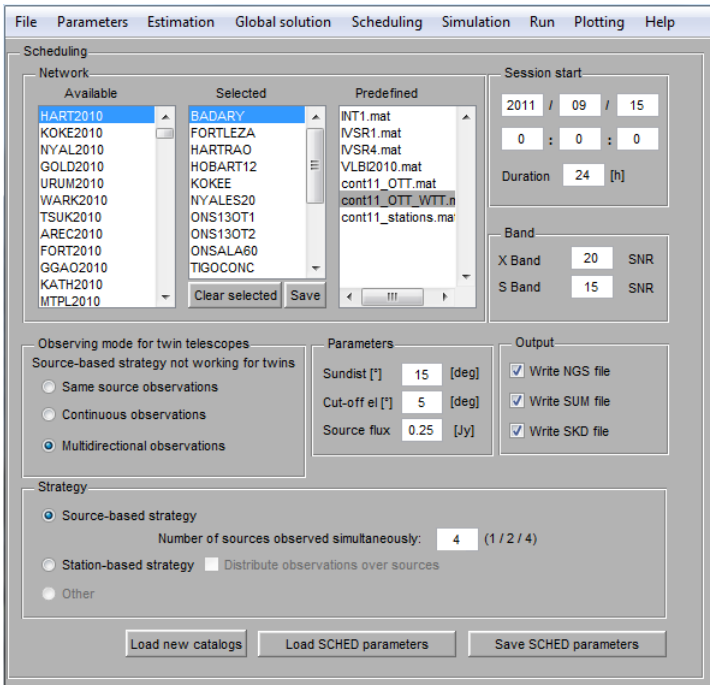

Figure 1.6: GUI of VieVS, where a scheduling is about to get started. The duration of the scheduling can be selected here, as well as the observing mode for TT together with the VLBI strategy among other things. The simulation which ensues in most cases is set up in a different tab.

Finally geodetic parameters can be estimated with a least squares method (LSM). These can be slant wet delays (usually every 60 minutes a day), troposphere gradients, clock parameters, and EOP among others [Schuh et al., 2010]. When a VLBI session is run in VieVS certain preferences for telescope strategies can be selected. Further details are delineated in the following chapter.

1.6.1 Scheduling strategies for VLBI Telescopes

Basically there are two main strategies for geodetic VLBI:

1. source-based strategy with two sources observed simultaneously

2. source-based strategy with four sources observed simultaneously

When the two source strategy is applied all participating telescopes in the network observe only two sources at a time (2 SAAT). Consequently the same applies to the four source observation (4 SAAT). The following figure shows the selection of sources of these strategies in a geometrical way (fig 1.7). The left delineation shows the two source strategy.

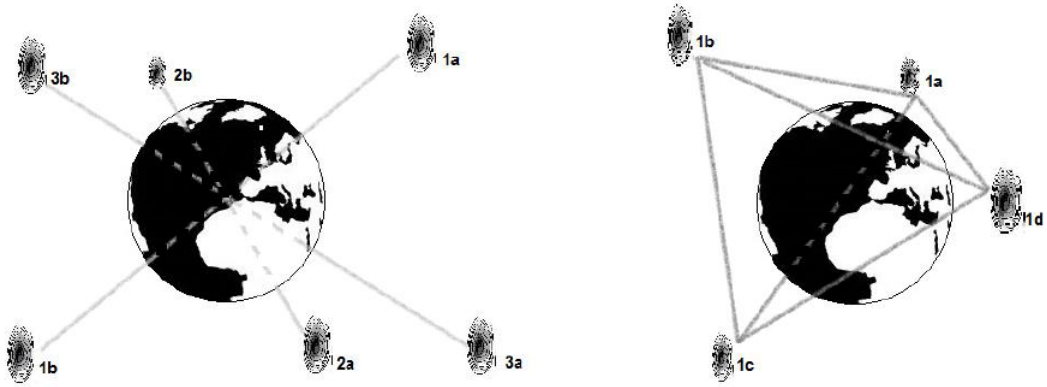

Figure 1.7: Selection of sources under two different strategies. On the left side the two source observation is depicted. The letters a and b each indicate the affiliation of the two sources, which are observed simultaneously. On the right side, four sources at a time are observed, described with the letters a to d. [Schönberger et al., 2015]

Obviously the two related sources, each indicated with a number, lie directly opposite the Earth. When these two sources are targeted, different subnets of antennas are formed. The minimum size for these subnets scheduled at a time is set to 25% compared to the entire VLBI network [Madzak et al., 2013]. With the 4 SAAT strategy more scans can be anticipated. The geometric array is shown on the right side of the figure. The more sources observed simultaneously the more subnets can be formed and adjusted. This should also lead to an increase in the accuracy of station positions, which will be discussed later.

1.7 Twin Telescopes

The single scans of each of the antennas linked as one TT are then united. Both of these single antennas must also have the same clock since they are a pair of identical antennas with the same hardware. Other characteristics are the accurately known local tie vector and the same atmosphere conditions for the telescopes, since they mostly are only a few hundred metres apart. Table 1.4 shows a few technical specifications of these telescopes. The smaller TT naturally perform faster movements and can therefore observe more quasars in shorter time.

Station	Diameter [m]	Horizontal slew rate [deg/sec]	Vertical slew rate [deg/sec]
ONSALA60	20.0	2.4	1.0
OTT	13.2	12.0	6.0
WETTZELL	20.0	3.0	1.5
WTT	13.2	12.0	6.0

Table 1.4: Technical specifications of the telescopes of Onsala (SWE) and Wettzell (GER) and their related TT. These are not official numbers.

1.7.1 Observation modes for Twin Telescopes

As mentioned above TT are capable of observing radio sources under different observation modes with each having its own idiosyncrasies. The following observation modes are eligible in the VieVS GUI [Sun et al., 2012]:

1. multidirectional observations
2. continuous observations
3. same source observations

Multidirectional observations follow their descriptions and are performed in all directions at every site having TT. Then different subnets of the entire VLBI network can be formed and adjusted. Further this also results in a higher number of observations per baseline compared to the other strategies.
In contrast to this the continuous mode always keeps one of the twins fixed at a source, whereas the other one slews to the next source. This assures continuous observations.
Lastly there is the same source observation, where both of the twins observe the same source. With this approach the scheduling programme selects radio sources for each station from the source catalogue which are independent of the source distribution [Sun et al., 2014]. This leads to an enhancement in sensitivity of the telescopes. The TT then work as one large telescope with a collecting area approximately twice as large compared to one of the twins. The same source observation mode also takes advantage of the shorter time to achieve the minimum Signal to Noise Ratio (SNR) of the source. This strategy has not been investigated in this study.
All of these observation modes can be conducted with one, two or four sources observed simultaneously, whereas this thesis treats only the last two cases. Logically more sources

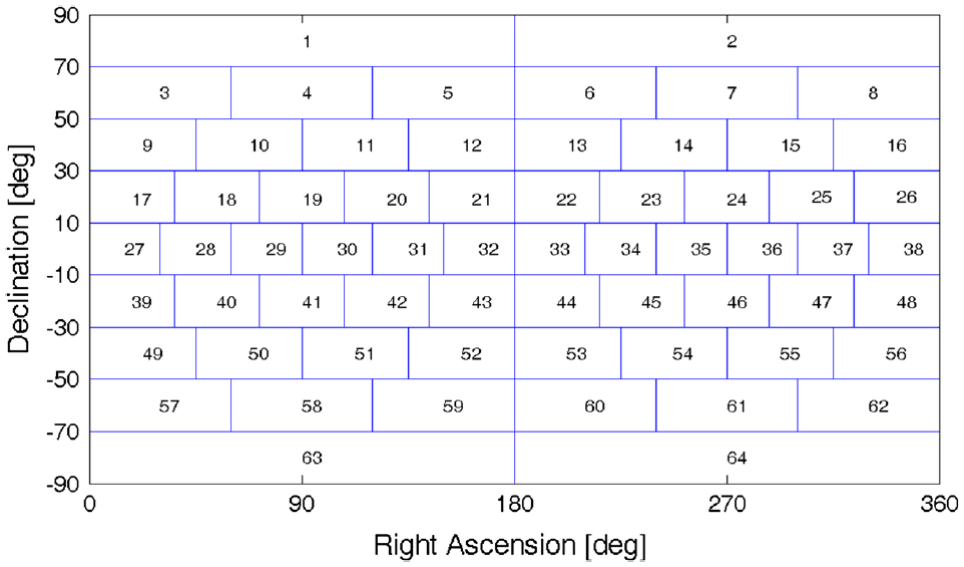

Figure 1.8: Distribution of sources on the celestial sphere. The declination interval is 20° and the right ascension interval is a function of declination. The number of observed sources is written in each segment.[Sun et al., 2014]

observed mean a higher number of scans which could potentially have an effect on the VLBI results. Figure 1.8 shows the source distribution on the celestial sphere in a certain time span [Sun et al., 2014]. Therefore the celestial sphere is segmented by right ascension and declination. The ordinate is split into a 20° interval, while the abscissa interval is a function of the declination. Only the segments with at least one source observed are of importance. The best possible distribution (100%) is achieved if each segment comprises the same number of observations. In contrast the distribution is 0% when all sources are located in one single segment. This approach has similarities to the skyplots which are shown when it comes to the results of the experiments.

2 Experiments with VLBI scheduling

The following experiments were executed to verify the results of the CONT11 VLBI campaign which was held in September 2011. Its aim was to determine station coordinates, EOP, and estimate the Earth's atmosphere among others. All this happened in coherency with high accuracy, low latency and high temporal solution. For the purpose of simulations with TT, CONT11 has been rescheduled and simulated with such telescopes at the sites of Onsala and Wettzell. These TT were added manually to the list of participating stations in VieVS and did not take part in the original CONT11 campaign.

2.1 Applied Schedules in VieVS

In addition to the two scheduling strategies for VLBI stations, the following observing modes merely for TT in Onsala and Wettzell are chosen during the scheduling:

1. multidirectional observations
2. continuous observations

Within these strategies and observation modes the following parameters for all stations have been set and never changed, while using different observing modes of the Twin Telescopes:

- min. sun-distance: 15 deg
- cut-off elevation: 5 deg
- min. source flux: 0.25 Jy

Stations	Observation mode of TT	Number of sources at a time
CONT11 incl. OTT & WTT	multidirectional	2 SAAT
CONT11 incl. OTT & WTT	multidirectional	4 SAAT
CONT11 incl. OTT & WTT	continuous	2 SAAT
CONT11 incl. OTT & WTT	continuous	4 SAAT

Table 2.1: VieVS setup for the scheduling of TT in Onsala and Wettzell. The observation modes are multidirectional and continuous with two and four sources observed at a time (SAAT).

The SNR of the telescopes is set to 20 and 15 for X-Band and S-Band respectively. All together there are four schedules carried out in VieVS which are summarised in table 2.1. In each schedule the thirteen CONT11 VLBI telescopes took part plus the Twin Telescopes in Onsala and Wettzell. All sessions started on the 15^{th} of September 2011 at 00:00:00 UTC and took 24 hours of scheduling. The reason for only one day of scheduling is that the source constellation in space alters only by 4 minutes from day to day with respect to the Earth. This is due to the Earth's movement according to sidereal days. Hence more days of scheduling would hardly deliver significant vantages in terms of estimated parameters, but demand a much longer calculation time.

2.2 Simulations

When the constellation between the 17 antennas and radio sources over a day is scheduled this single day is simulated with 25 realisations. In the further course the atmosphere and its behaviour are simulated for these days. The results are so-called Slant Wet Delays (SWD). They represent the signal delays of the atmosphere measured from each antenna towards the observed sources. For better modelling and comparison of the layers above the ground the SWD are mapped into zenith direction. The resulting parameters are Zenith Wet Delays (ZWD). The mapping of the slanted signal is done via mapping functions. Moreover certain corrections are taken into account for the simulations to make them more accurate and reasonable. These corrections include tidal atmosphere loading, tidal ocean loading, solid Earth tides, and ocean pole tide loading.

Pany et al. simulate the impact of the three main stochastic error sources in VLBI on station positioning [Pany et al., 2010]. These are both fluctuations of the wet troposphere

delay and station clocks, and measurement errors in the VLBI system. Therefore Monte Carlo simulations are run where each of these parameters is varied while the others are kept fixed. This results in the final outcome that the troposphere has the largest impact, if not modelled correctly. More precisely it is the wet refractive structure constant Cn, the effective height of the wet troposphere H, and the wind speed v towards East. All of these parameters are described in more detail in the following chapter. The bottom line is that this atmospheric layer gets the most attention regarding error influences in this thesis. Finally VieVS is also capable of simulating station clocks, white noise, and the source structure. The latter is not taken into account for the simulations however.

2.2.1 Turbulence parameters

To simulate ZWD in the course of the VLBI adjustment, certain parameters have to be set for the simulation in advance. These are the turbulence parameters H, vn and ve. Where H is the scale height of the troposphere and the last two are wind velocities towards North and East. Moreover there are the a priori zenith wet delay *wzd0*, a correlation interval *dhseg* and the step width for the numerical integration *dh*. Lastly there are parameters which are set for clock simulations. These are the clock Allan Standard Deviation ASD at 50 minutes after the beginning of the recordings and the white noise *wn*. The values of these parameters and their units can be found in table 2.2.

Simulation parameter	Value	[unit]	
H	2000	$[m]$	for troposphere
vn	0.0	$[m/s]$	
ve	8.0	$[m/s]$	
wzd0	250	$[mm]$	
dhseg	2	$[h]$	
dh	200	$[m]$	
ASD	10^{-14} @ 50 min	[ ]	for Clocks
wn	32	$[ps]$	

Table 2.2: Simulation parameters which count for all stations. H is the scale height of the troposphere, vn and ve are wind velocities towards North and East, respectively. *wzd0* is an a priori zenith wet delay, *dhseg* is a correlation interval, *dh* represents the step width for the numerical integration. Parameters for clock simulations are represented by the clock Allan Standard Deviation ASD at 50 minutes after start and the white noise *wn*.

The most important parameter is *Cn* however. It is an additional turbulence parameter and the only one which is assumed to be site dependent. These *Cn* values were derived from GPS measurements in the year 2011 [Nilsson and Haas, 2010]. All *Cn* values for the stations taking part in the simulation are shown in table 2.3.

Station name	Cn [$10^{-7}\ m^{-1/3}$]	Station name	Cn [$10^{-7}\ m^{-1/3}$]
BADARY	1.37	WESTFORD	2.30
FORTLEZA	2.46	WETTZELL	1.50
HARTRAO	1.34	YEBES40M	1.48
HOBART12	1.60	ZELENCHK	1.86
KOKEE	1.39	ONS13OT1	2.19
NYALES20	0.65	ONS13OT2	2.19
ONSALA60	2.19	WETTZTT1	1.50
TIGOCONC	2.08	WETTZTT2	1.50
TSUKUB32	3.45		

Table 2.3: Atmospheric turbulence parameters for all stations taking part in the VLBI scheduling in VieVS. The Twin stations in Onsala, ONS13OT1 and ONS13OT2, and Wettzell, WETTZTT1 and WETTZTT2, are pooled to one Twin Telescope on each site during the calculations.

The Japanese station TSUKUB32 has the largest turbulence parameter, while NYALES20 in Norway has the lowest. This is not surprising, since the former station is closer to the equator while the Norwegian station is the farthermost and atmospheric turbulences are higher in lower latitudes. All other simulation parameters apply to all stations.

2.3 Least Squares Adjustment

Right after the simulation over 25 days an adjustment is performed. With the least squares adjustment station positions are estimated and Baseline Length Repeatabilities (BLR) are calculated out of the coordinates as a measure of position accuracies as described in 1.2.9. The resulting outcomes are discussed in the following chapter.

Finally this study will also enter into the question whether there is a link between a higher number of observations and scans at the Twin Telescope's sites and better BLR together with higher accuracies for station coordinates. If so, creating TT will pay off hopefully within the next years.

3 Results of VLBI scheduling

This chapter presents the results of the different schedules, observing modes and strategies with the TT from chapter 2. As a reminder, these observing modes are:

- multidirectional observations with two sources at a time
- multidirectional observations with four sources at a time
- continuous observations with two sources at a time
- continuous observations with four sources at a time

After all this study should demonstrate which schedules and related observing modes of TT perform best in the final VLBI analysis.

3.1 Number of scans and observations

As a matter of fact TT have a faster slewing rate due to their more compact construction. Therefore they are capable of observing more radio sources in space compared to existing telescopes. This circumstance shall be shown by means of the scans and observations of the telescopes . A scan is a direct survey of one telescope to one source at a time. A source now can also be observed by several telescopes each performing a scan of the same source. To paraphrase several scans from different telescopes to the same source complete an observation. Figure 3.1 and figure 3.2 show the number of those for four selected telescopes under four different observation modes in the scheduling. Scanning four sources at a time in both multidirectional and continuous mode results in the highest numbers of scans for both TT. Regarding the amount of observations it can clearly be seen that they are higher at the TT's sites compared to the original ones under all four

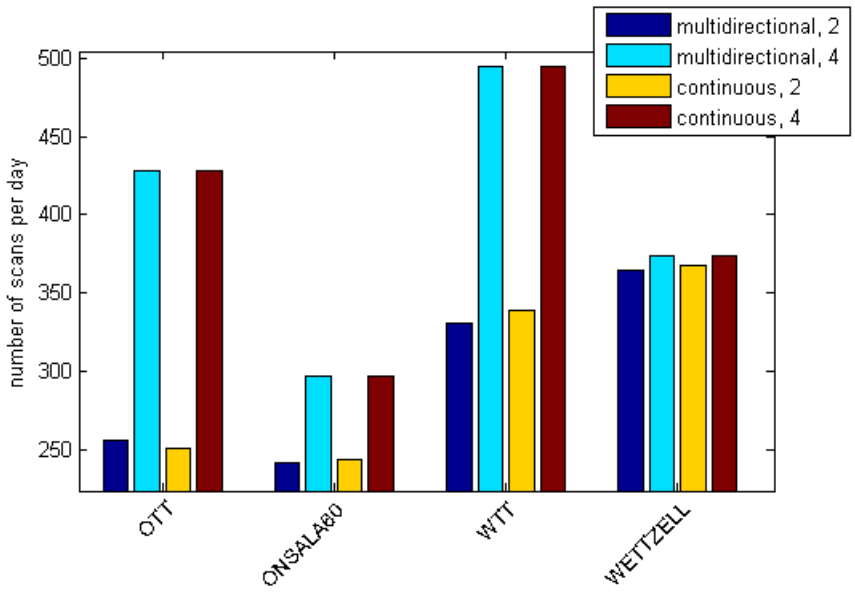

Figure 3.1: Number of scans on every simulated day for the stations OTT, Onsala60, WTT and Wettzell.

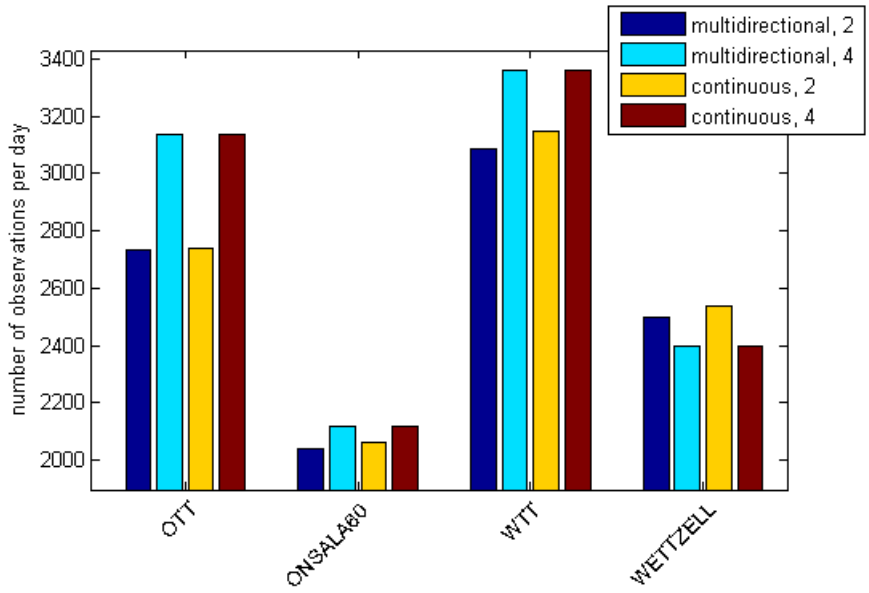

Figure 3.2: Number of observations on every simulated day for the stations OTT, Onsala60, WTT and Wettzell.

observations modes. It is the case that the number of simultaneously observed sources is an essential factor. The observation mode for TT is not so important though, concerning the number of scans and observations.
The twins in Onsala both perform more scans and observations than the 60 feet antenna. Even if the number of direct scans is only a little more, it is an expected outcome. In contrast to this the number of scans of the Wettzell TT is actually lower when two sources are observed at a time compared to their nearby counterparts. This fact is surprising in any case. It means that the WTT scans participate in many subnets to form observations. The absolute number of single scans is low though. Under the two source strategy TT show no related benefits. The more sources are used, the better for the twins. A direct comparison of the two source strategy with the later described BLR and ZWD is not expedient here, since the latter only relate to strategies with four sources.

3.2 Observation Time

It is not only the quantities of scans and observations which give a measure of how good the atmosphere can be simulated. It is also their temporal distribution over a scheduled day. Basically a higher number of scans guarantees a high dissolving model of the atmosphere, but simulating even more realistically requires scans of a day at all times. This is essential because the atmosphere's behaviour alters distinctly in 24 hours. To achieve this equally temporal distribution of scans, the scheduling programme ensures no telescope is idle for more than six minutes during the day. Table 3.1 shows the observation times in percent of the one scheduled day with four selected telescopes during four different observing modes. As it can be seen TT are consistently more occupied than their larger counterparts.

	observing mode			
	2 SAAT		4 SAAT	
Telescope	MD	CO	MD	CO
OTT	47	45	56	39
ONSALA60	41	40	33	33
WTT	43	50	62	39
WETTZELL	23	22	19	20

Table 3.1: Observation time in percent of four selected telescopes during the scheduled day of the CONT11 campaign. *MD* stands for the multidirectional observation mode and *CO* for the continuous one.

3.3 Distribution of scans

To further examine the results of previous VLBI sessions the distributions of radio sources in the sky can be investigated more accurately. This can be achieved best by polar plots of all scans of a single station, which are carried out each day during the simulation. The only constraints for scans which are set up in advance are a minimum elevation of 5 deg. above horizon and 15 deg. Sun distance. Figure 3.3 and fig. 3.4 illustrate the skyplots of the four main stations. The outer circle represents the scan azimuth in geodetic negative orientation. The inner circles represent the zenith distance. All circles are scaled in degrees. According to the settings in VieVS low elevation scans are excluded from the sessions.
In the case of Sweden the observation mode is multidirectional with four SAAT. The German antennas show the sky coverage under the continuous mode with 4 SAAT also. One characteristic that stands out of these plots straight away are the holes on the north side. These holes are in alignment with the north holes from GPS-satellite skyplots over a day, whereas there are no such constraints applied in this case. This suggests that the used algorithm for scan distributions is in need of improvement. Apart from these gaps the quantities and distributions are good for scans in all directions and elevations. This implies that the atmosphere can be simulated in very realistic ways, eminently at stations with TT. Further investigations show that this gap randomly appears at certain sites, but not at all of them. It is independent from the observation mode and therefore it can appear in all four of them.

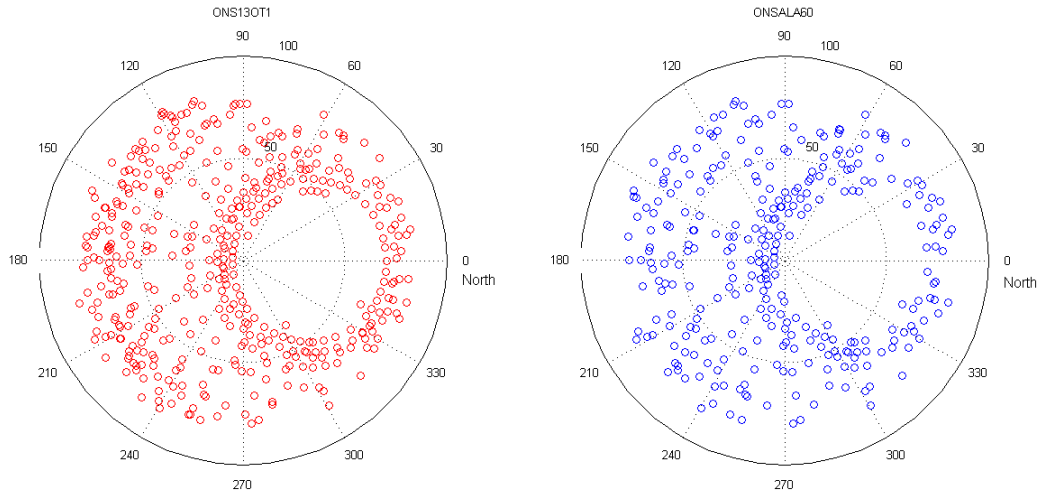

Figure 3.3: Distributions of 428 Scans of ONS13OT1 and 297 Scans of ONSALA60. The observing mode is each multidirectional with four SAAT.

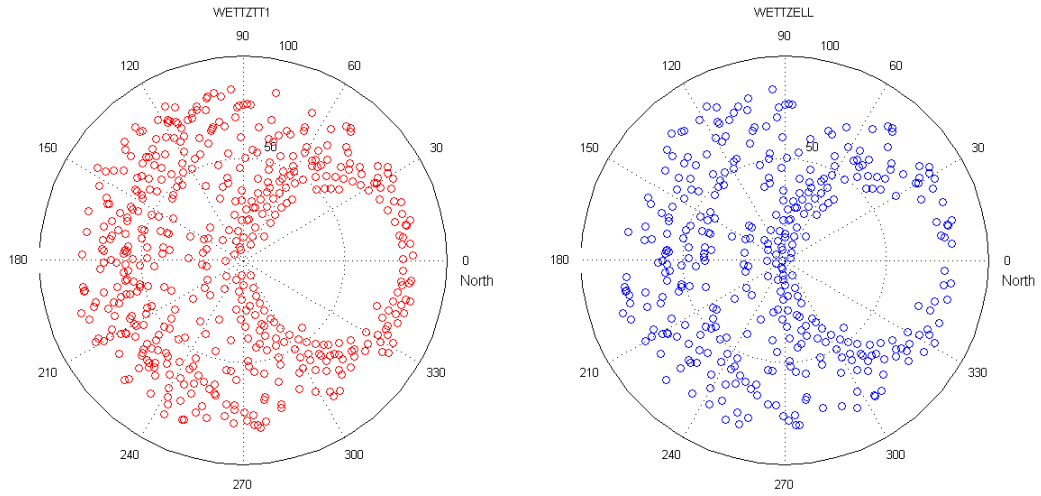

Figure 3.4: Distributions of 495 Scans of WETTZTT1 and 374 Scans of WETTZELL. The observing mode is each continuous with four SAAT.

Figure 3.5 shows the sky coverage of the Australian station HOBART12 and of the Chilean station TIGOCONC in two different observation modes by way of comparison. There is no pattern to identify a dependence regarding the northern or southern hemisphere. It is not clear why VieVS produces such significantly different distributions of the scans. A possible explanation could be that sources in that direction radiate with a too low flux density and therefore are not detected. Alternatively the source catalogue north of Onsala is not entirely complete. In fact VieVS is still under construction with respect to scheduling TT.

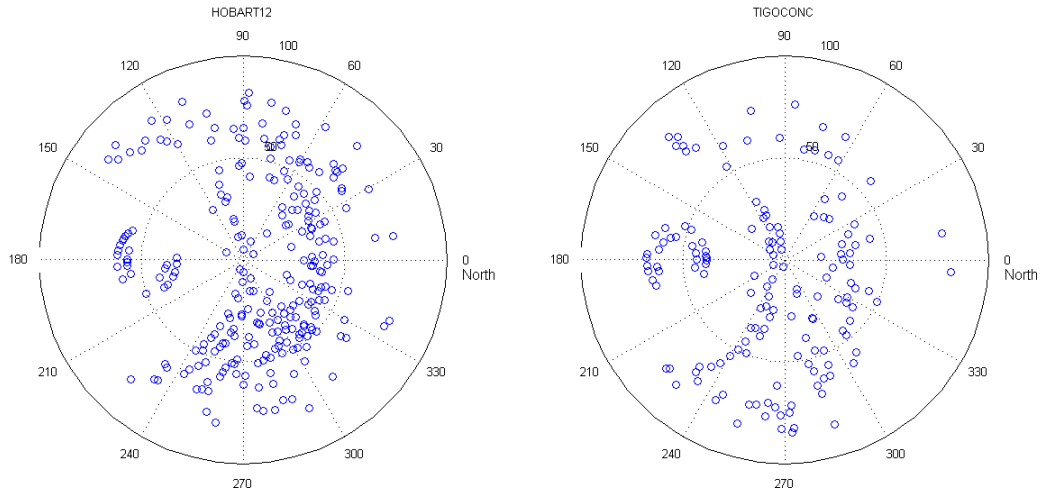

Figure 3.5: Sky coverage of HOBART12 and TIGOCONC each day. Four sources are observed simultaneously in multidirectional and continuous observation mode respectively.

3.4 Atmospheric delays

In order to get a representative measure of the atmospheric turbulences over each station VieVS is capable to simulate and estimate the effects of the Earth's atmosphere on incoming radio signals. These effects can be described on the basis of atmospheric delays. More precisely the delays are slant wet delays (SWD) in straight direction to the quasars. These SWD are divided by the Vienna Mapping Function (VMF) to receive zenith wet delays (ZWD). As the name implies these ZWD describe the delay of the signal path in zenith direction at each station. A simulation is done in advance of the network's adjustment, whereas the estimated zenith delay (ZD) values arise as a direct result of the adjustment. Moreover there is a different number of these two kinds of ZD. During the simulation over 25 days, telescopes perform hundreds of scans. The exact amount of them, however, depends on the observation mode and the number of sources observed simultaneously. That is why the amount of these two kinds of ZD values must be brought into alignment, which is done by interpolation. In this case the estimated ZD are interpolated towards the simulated values. As a result of the interpolation there are now a few hundreds of ZD values available for each station.

The following four figures show ZD before and after the adjustment (simulated and estimated respectively) for four selected antennas. For reasons of simplification only the multidirectional observation mode with four sources at a time (SAAT) is investigated. For the VLBI sessions ZWD are estimated every 60 minutes and relative constraints between ZWD offsets are set to 1.5 cm after 60 minutes. Gradients in north and east direction are estimated every 360 minutes.

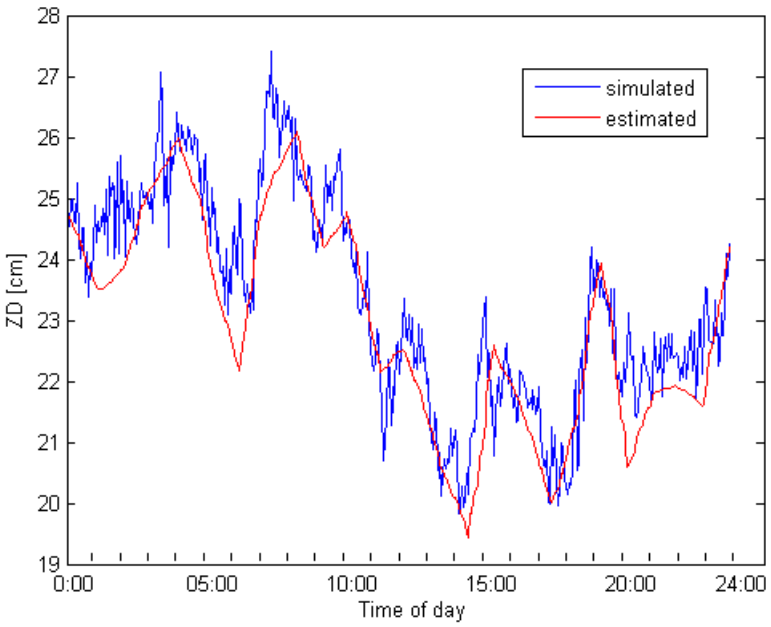

Figure 3.6: Simulated (blue) and estimated (red) ZWD of the TT in Onsala on the first simulated day. The observation mode is multidirectional with four sources observed simultaneously.

Figure 3.6 shows the ZD of the TT in Onsala during the first simulated day. The lowest ZD values appear in the afternoon but there are also the greatest fluctuations during this time. Three peaks and valleys each can be counted from 12 pm to around 8 pm, all randomly generated during the simulation.

Sometimes the correlation between the two data sets is not very high. This can be caused by the interpolation. As already mentioned the estimated ZD are interpolated towards the simulated values. They are even extrapolated towards the time stamps of the simulated ZD. Since the latter have several hundred values, the time window of the estimated ZD is too long and may cause these differences. This effect can be seen in subsequent ZD graphics even more clearly. All in all this station has the lowest ZD values on average compared to all four antennas which are investigated in more detail. Figure 3.7 shows the atmospheric delays of the ONSALA60 antenna located next to the TT on the west coast of Sweden. This time the ZD values move more regularly in the same magnitude throughout the day. The size difference between morning and afternoon is no longer as great as with the twins. Figure 3.8 shows the delays of the twins in Wettzell. Here the greatest delays are between 4 pm and 10 pm. Furthermore a huge interpolation error can be detected at 5 pm.

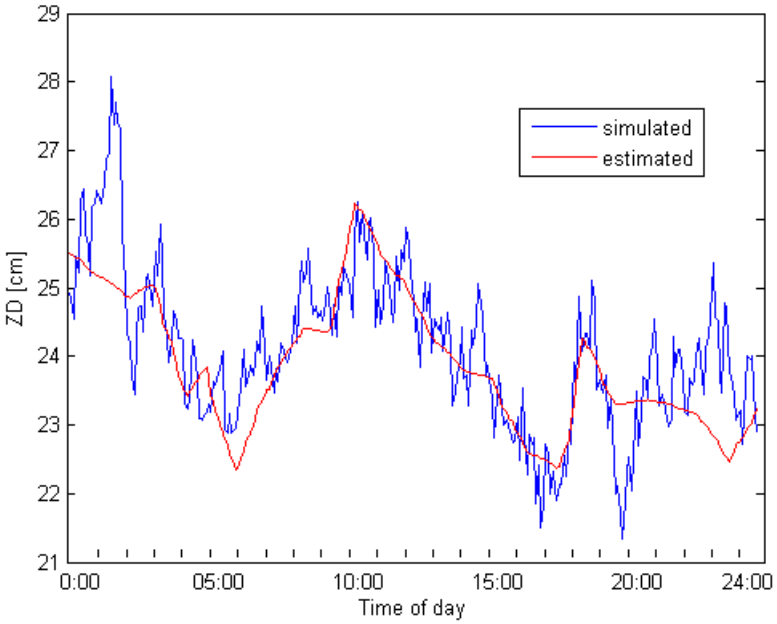

Figure 3.7: Simulated (blue) and estimated (red) ZWD of the ONSALA60 telescope on the first simulated day. The observation mode is multidirectional with four sources observed simultaneously.

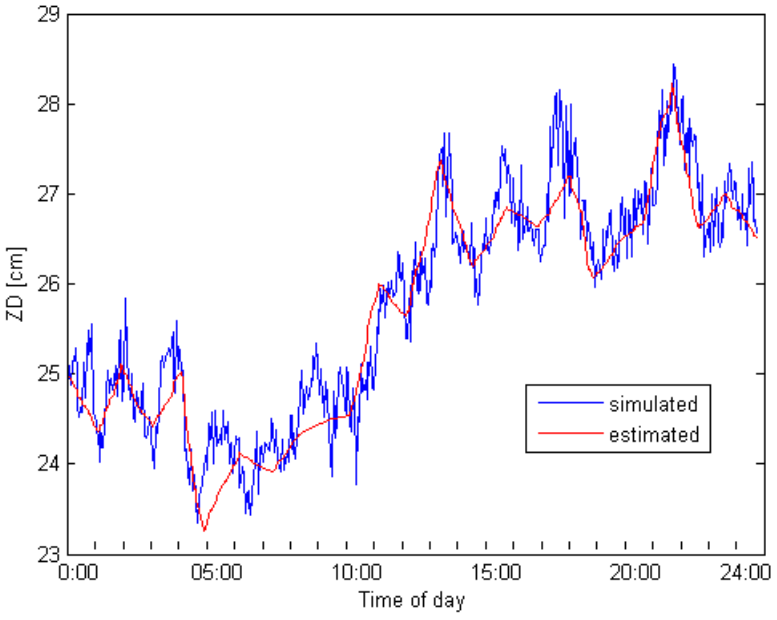

Figure 3.8: Simulated (blue) and estimated (red) ZWD of the TT in Wettzell on the first simulated day. The observation mode is multidirectional with four sources observed simultaneously.

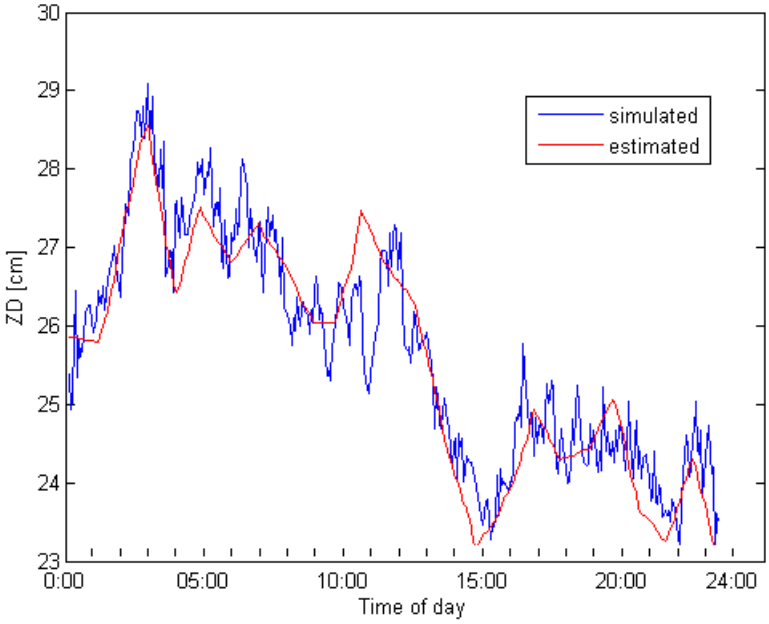

Figure 3.9: Simulated (blue) and estimated (red) ZWD of WETTZELL on the first simulated day. The observation mode is multidirectional with four sources observed simultaneously.

WETTZELL is the last station which is used for a comparison of the atmospheric delays (fig. 3.9). An outstanding feature is the large ascent of ZD at the beginning of the day. It also comprises the scans with the greatest delays of all. Some are up to 29 cm at 03:00 am. Compared with the TT in Wettzell the larger station also has the larger delays. Compared with the ONSALA60 telescope both stations exhibit a sharp increase of delays in the first two hours of the day. In the course of the day, however, the delays of both station drop down, where ONSALA60's delay are spread much more constantly over the whole day. In general the Swedish telescope achieves lower delays.

A comparison of the sites of Sweden and Germany shows that the stations in Onsala feature lower delays than the ones in Wettzell. This atmospheric investigation however only applies to the multidirectional strategy with 4 sources, which has been studied here. Other strategies may lead to different results.

3.4.1 Mean standard deviation of zenith delays

To add a degree of accuracy the standard deviation is considered. First the differences between the simulated and estimated ZD are calculated on each of the 25 days. As already mentioned the estimated ZD are interpolated towards the simulated ones. Then the standard deviation is applied to these ZD differences on each simulated day. This results in one value for every single day. Finally the mean value over these 25 standard deviations is calculated to deliver one final value. The entire process can be applied to every outcome of any scheduling with any observation mode. The following figures show the resulting plots represented by the stations in Onsala and Wettzell respectively. These sites are the only ones which are equipped with TT in the VLBI analysis. As expected TT deliver the higher

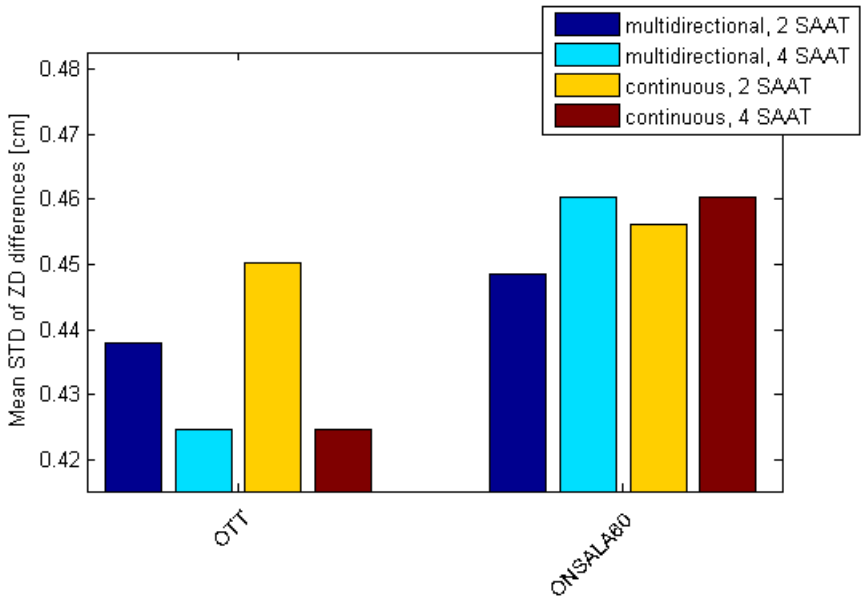

Figure 3.10: Mean standard deviation of simulated and estimated ZD differences over all 25 simulated days for the stations in Onsala.

accuracies regarding atmospheric turbulences (fig. 3.10). Especially when four sources are observed at the same time, the highest accuracies can be achieved. For the TT there is no difference in the observation mode when it comes to the investigation of four sources. Their accuracies are almost identical. Multidirectional observations perform better with two sources. The twins' continuous observation of two radio sources at a time features the worst accuracy of the atmosphere.

The observation mode, however, does not carry too much weight for the larger ONSALA60 station, it only applies to the TT in the scheduling. This means that these results show

no major disparities. Figure 3.11 shows the same statistics for the stations in Wettzell. In

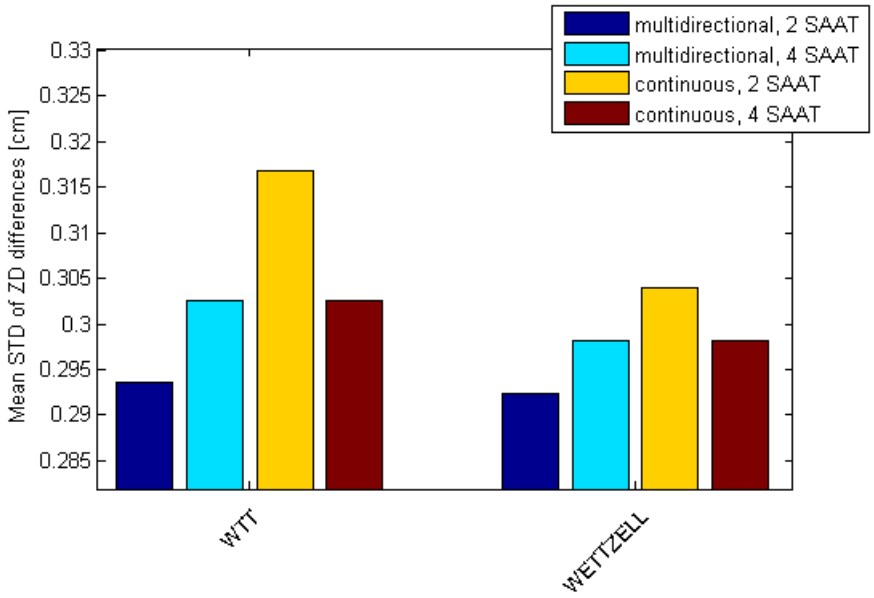

Figure 3.11: Mean standard deviation of simulated and estimated ZD differences over all 25 simulated days for the stations in Wettzell.

this case the larger telescope has a lower scattering of the delays in all observation modes. The multidirectional observation mode with two SAAT performs best for both antennas, while the continuous mode has the greatest standard deviation. The number of observed sources of the TT is here no longer of great importance.

3.5 Baseline Length Repeatability

To analyse the accuracy of station coordinates over the course of the adjustment the BLR can be investigated. These BLR are deduced directly from the adjusted station coordinates computed in VieVS. According to the initial scheduling strategies (table 2.1 in chapter 1.6.1) there are four different resulting plots for such BLR.

Figure 3.12 shows the BLR for the stations Onsala60, OTT, Wettzell, and WTT with multidirectional observations and two SAAT. The standard deviations of shorter baselines are slightly better for the OTT compared to its larger counterpart. Albeit there are also baselines with lengths around 8.000 km where the opposite is the case. Even longer baselines don't show improvements in their standard deviations in terms of the TT in Onsala. This is an unexpected result. It is assumed that the OTT feature a constantly smaller

BLR than their larger opposite. On top of that there is a similar situation between the German antennas. A reason for this could be that because there are TT, their observations with other telescopes experience a higher weight in the adjustment. This leads to the case that observations with no TT have a lower weight, or are conducted in the scheduling more rarely. TT can also attract more observations because there are two single antennas at each

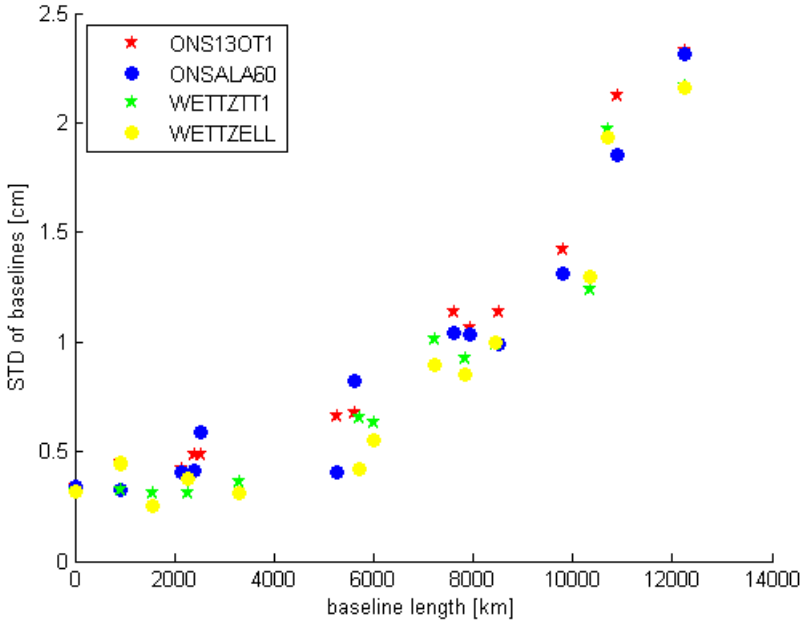

Figure 3.12: BLR for the stations Onsala60, OTT, Wettzell and WTT. The observation mode is multidirectional with two SAAT.

site. Therefore they have more scans and observations in time than other stations. These stations experience less observations or even none. The continuous mode with two SAAT, however, behaves differently for baselines at 8.000 km length. The twins in Onsala appear to have lower standard deviations than the ONSALA60 station, whereas the accuracies are almost equal at the sites in Wettzell (fig. 3.13). In general BLR are greater at 8.000 km compared to the multidirectional observation mode with two SAAT. There is one outlier in the observations of the German stations, however. It is the baseline to HARTRAO in South Africa. Other outliers appear at distances of 10.000 km and 12.000 km. These are the stations in Chile (TIGOCONC) and Tasmania (HOBART12).

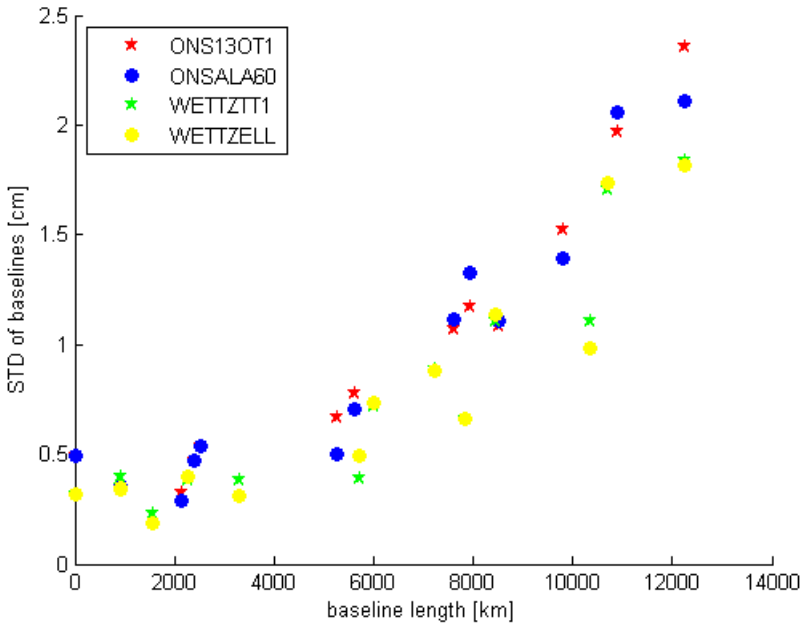

Figure 3.13: BLR for the stations Onsala60, OTT, Wettzell and WTT. The observation mode is continuous with two SAAT.

It is also possible that certain outliers preponderate at longer baselines. Especially to the last two mentioned stations only a few baselines are scheduled under all four strategies. The stations present less than 20 observations and in some cases there are even less than 10. That is a relatively low number, since usually between 100 and 200 observations are conducted with other stations. These two stations are already noticed by a lower density of scans. There may also be a correlation to the distribution of the scans (figure 3.5 on page 37). In general the German telescopes consistently present better BLR than the ones on Sweden.

The following two plots (fig. 3.14 and fig. 3.15) refer to both observation modes (multidirectional and continuous) with four sources observed simultaneously. These strategies show very unique behaviours of standard deviations. For baselines with lengths less than 10.000 km their repeatabilities are in a magnitude which is lower than the 2 source strategies. The order of magnitude is 1.3 cm or lower. Longer baselines, however, feature a completely different behaviour in their accuracies. Their standard deviations are even higher on average than in the two source strategy. There is a clear saltus in the pattern of standard deviations at around 11.000 km. These long baselines all have a standard deviation of clearly more than 2 cm. The baseline with the worst standard deviation is spanned between ONSALA60 and HOBART12.

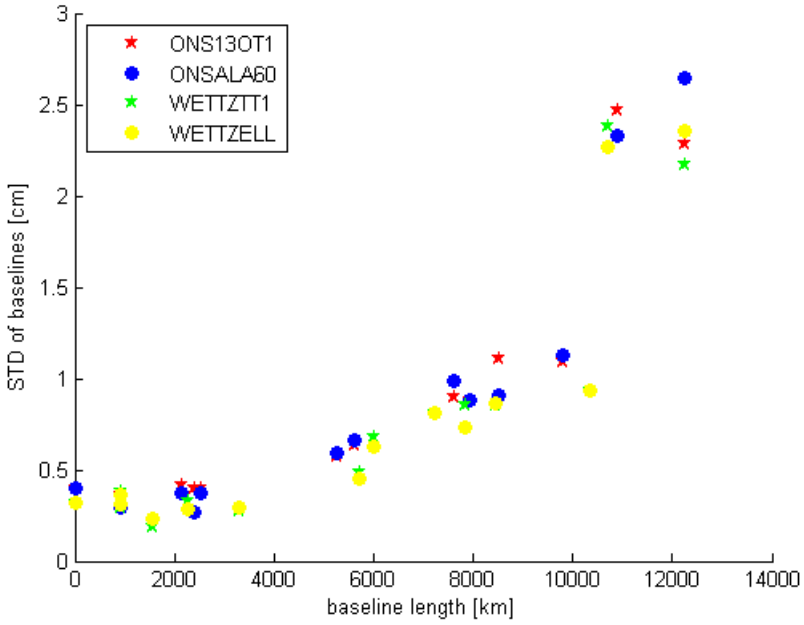

Figure 3.14: BLR for the stations Onsala60, OTT, Wettzell and WTT. The observation mode is multidirectional with four SAAT.

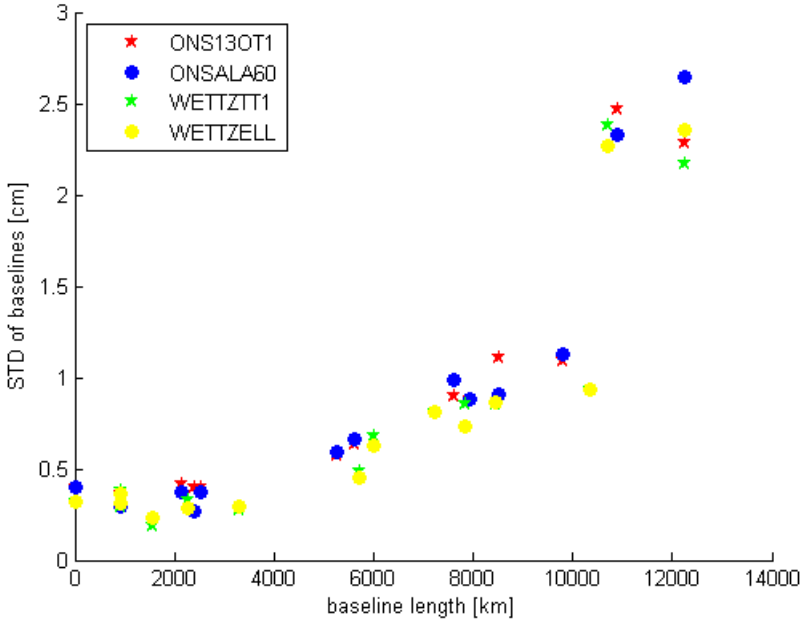

Figure 3.15: BLR for the stations Onsala60, OTT, Wettzell and WTT. The observation mode is continuous with four SAAT.

Generally it can be said that with the scheduling package of VieVS there is no significant improvement with the use of TT in terms of BLR. This stands in direct contrast to the previously assumed benefits of using TT in VLBI scheduling. A comparison between these telescopes and other antennas was not made in the course of this thesis. Further profound studies may give more indication. The order of magnitude of all standard deviations is on a reasonable scale however.

4 Conclusion

The upshot of this study about VLBI-TT is ambiguous. With VieVS they don't show their expected advantages in all evaluated areas compared to the previously existing antennas. The true advantages of TT lie in the sky coverage most evidently. TT deliver a significant improvement in treating the atmosphere due to their higher number of scans. This leads to a better zenith wet delay estimation at the stations. The TT in Onsala feature lower atmospheric standard deviations than their larger counterparts, whereas a difference is far harder to identify at the German antennas. To further enhance atmospheric estimations a reduction of its estimation interval from 60 minutes to 20 minutes is aspired, together with simulations lasting even longer than 25 days.

Surprisingly the BLR of stations with TT don't show significant improvements in terms of accuracies. Nevertheless with higher numbers of scans and observations the active time of each telescope can be increased and therefore a better distribution of the sky is obtained. That is to say that outliers do preponderate less, when more baselines are calculated. A link to the stations sky coverage can also be discovered. This accounts for both sites.

Furthermore it is hard to tell if there is an ideal strategy for TT in VieVS. The multidirectional observation mode is most likely to be used for atmospheric modelling. In this case the atmosphere is best rayed in all directions. Nevertheless the continuous observations result in a greater number of scans for the German stations. This mode will also pay off the more TT are in a VLBI network.

To show further advantages of the TT pervasive research is inevitable. That is to say that studies need to be conducted over a more extended period of time.

The twins in Onsala are expected to operate unlimitedly in 2017 and will make their contribution to VIGOS' goals. This means achieving precisions of 1 mm in station position and 0.1 mm/yr in station velocity. Further VIGOS projects including these new types of radio telescopes will be realised within the next years.

5 Outlook

The IVS proposed a path to the next generation VLBI system with unequalled new capabilities: increasing position and velocity accuracy to 1 mm and 0.1 mm/yr on global scales, consistent time series of station positions and Earth orientation parameters, and a fast delivery of initial geodetic results within 24 hours. Therefore the VLBI2010 Committee (V2C) was initiated to conduct studies and to propel the realisation of this new vision for geodetic VLBI. In the course of these projects the development of Monte Carlo simulators served to study main VLBI random error processes, such as the atmosphere, clocks and noise, and approaches for their reduction, like shortening the source switching interval, were aspired. In all cases the Monte Carlo simulators declared the troposphere as the dominant error source. That is why the investigation of the atmosphere is a main priority of the IVS [Pany et al., 2010].

Reducing the observing time of a radio source requires a trade-off between measuring the delay under high accuracy together with the sufficient SNR. To manage this balancing act widely spaced frequency bands are in use to solve the interferometric phase. These are called broadband delays. The new frequency range will span 2 to 14 GHz recordable in four bands combined with a data rate of 32 GB/sec and a transmission rate of up to 8 GB/sec. These high rates are necessary to observe a sufficient amount of radio sources for VLBI [Petrachenko et al., 2009].

IVS' progress report suggests the erection of antennas linked via high speed fibre networks to provide initial IVS products within 24 hours after observation. Also IVS prioritises the buildout of stations in the Southern hemisphere to reach a balance between next-generation antennas and current receiving systems. Another step towards the future is enhanced automation of the stations and analysis processes. This favours the reduction of operating costs. The antennas can be monitored and operated centrally to improve operating modes and updates schedules accordingly [Petrachenko et al., 2009].

Regarding TT they will pay off, the more there are around the globe. This means more baselines can be calculated and the atmosphere can be estimated and predicted more realistically. Single scans with TT also have their advantages with lower slewing times, but these are by far not as great as if there were at least two or more at different sites. Moreover the same source observation mode as well as the continuous observation mode are expected to become more beneficial for TT [Sun et al., 2012].

TT south of the equator will also contribute to estimate the atmosphere more accurately due to a better distribution of the antennas. So far Wettzell is the only site with operative TT. Onsala's TT are expected to be fully operational in 2017. These two TT together with future antenna projects will make their ongoing contribution to the realisation of global geodetic reference frames and orientation of the Earth in space among other geodetic tasks in the future. Further TT are planned or under construction already including the site of Ny-Ålesund in Norway.

List of Figures

1.1 Wettzell antenna 6
1.2 Flow diagram of geodetic VLBI 9
1.3 Geometric concept of VLBI 11
1.4 Air view of the Onsala Space Observatory 20
1.5 Distribution of participating VLBI stations in the CONT11 campaign . . . 21
1.6 Graphical User Interface of VieVS 24
1.7 Two and four SAAT geometry 25
1.8 Celestial sphere grid with source distribution 27

3.1 Number of scans for OTT, Onsala60, WTT and Wettzell 33
3.2 Number of observations for OTT, Onsala60, WTT and Wettzell 33
3.3 Skyplots of ONS13OT1 and Onsala60 in multidirectional observation mode with four SAAT 36
3.4 Skyplots of WETTZTT1 and WETTZELL in continuous observation mode with four SAAT 36
3.5 Skyplot of HOBART12 and TIGOCONC with four SAAT observation mode 37
3.6 Simulated and estimated ZWD of OTT in multidirectional observation mode with two SAAT 39
3.7 Simulated and estimated ZWD of ONSALA60 in multidirectional observation mode with four SAAT 40
3.8 Simulated and estimated ZWD of WTT in multidirectional observation mode with four SAAT 40
3.9 Simulated and estimated ZWD of WETTZELL in multidirectional observation mode with four SAAT 41
3.10 Mean STD of ZD differences for the stations in Onsala 42
3.11 Mean STD of ZD differences for the stations in Wettzell 43

3.12 BLR for Onsala60, OTT, Wettzell and WTT in multidirectional observation mode with two SAAT 44
3.13 BLR for Onsala60, OTT, Wettzell and WTT in continuous observation mode with two SAAT 45
3.14 BLR for Onsala60, OTT, Wettzell and WTT in multidirectional observation mode with four SAAT 46
3.15 BLR for Onsala60, OTT, Wettzell and WTT in continuous observation mode with four SAAT 46

List of Tables

1.1 Geodetic space techniques and their capabilities 5
1.2 14 Frequency Channels of data acquisition 7
1.3 New VGOS antenna specifications 22
1.4 Technical specifications of Onsala and Wettzell 26

2.1 Scheduling and observation modes of Twin Telescopes 29
2.2 Simulation parameters for all stations 30
2.3 Turbulence parameters for all stations of the VLBI scheduling in VieVS . . 31

3.1 Observation time of telescopes during CONT11 35

6 Acronyms

ASD	Allan Standard Deviation
BLR	Baseline Length Repeatability
CIO	Celestial Intermediate Origin
CIP	Celestial Intermediate Pole
CO	continuous observing mode for Twin Telescopes
DORIS	Doppler Orbitography and Radiopositioning Integrated by Satellite
dUT1	length of day, equals time difference between UT1 and UTC
EOP	Earth Orientation Parameters
FCN	Free Core Nutation
FORTLEZA	Brazilian VLBI station (14,2 m in diameter).
GNSS	Global Navigation Satellite System
GPS	Global Positioning System
GUI	Graphical User Interface
HOBART12	Australian VLBI station (26 m in diameter), located in Tansania.
ICRF	International Celestial Reference Frame

IERS	International Earth Rotation and Reference Systems Service
ITRF	International Terrestrial Reference Frame
ITRS	International Terrestrial Reference System
IVS	International Service for Geodesy and Astrometry
LEO	Low Earth Orbiter
LLR	Lunar Laser Ranging
LSM	Least Squares Method
MD	multidirectional observing mode for Twin Telescopes
MF	Mapping function
NNR	no-net-rotation
NNT	no-net-translation
ONS13OT1	first of the two Onsala Twin Telescopes
ONS13OT2	second of the two Onsala Twin Telescopes
OSO	Onsala Space Observatory
OTT	Onsala Twin Telescopes
RMS	Root Mean Square
SAAT	source at a time
SEFD	System equivalent Flux Density
SLR	Satellite Laser Ranging

SNR	Signal Noise Ratio
STD	Standard deviation
TAI	International Atomic Time
TIO	Terrestrial Intermediate Origin
TT	Twin Telescope
UT1	Universal Time 1
UTC	Universal Time Coordinated
VGOS	VLBI2010 Global Observing System
VieVS	Vienna VLBI Software
VM1	Vienna Mapping Function for hydrostatic and the wet delays of the atmosphere
VLBI	Very Long Baseline Interferometry
WETTZTT1	first of the two Wettzell Twin Telescopes
WETTZTT2	second of the two Wettzell Twin Telescopes
WTT	Wettzell Twin Telescopes
ZD	Zenith Delay
ZWD	Zenith Wet Delay

Bibliography

Inc Advameg. 2015. URL http://www.scienceclarified.com/Qu-Ro/Quasar.html.

British Astronomical Association. Radio astronomy group. 2011. URL http://www.britastro.org/radio/RadioSources/overview.html.

C.C. Bare, B.G. Clark, K.I. Kellerman, M.H. Cohen, and D.L. Jauncey. Interferometry experiment with independent local oscillators. *Science*, page 157, 1967.

S. Böckmann, T. Artz, and A. Nothnagel. VLBI terrestrial reference frame contributions to ITRF2008. *J. Geod.*, 84:201–219, 2010.

Johannes Böhm. Atmospheric Effects in Geodesy, lecture notes. 2012.

INC Computational Physics. 2014. URL http://www.cpi.com/projects/vlbi.html.

V. Dehant and P.M. Mathews. Earth rotation variations. in T.A. Herring, ed.,. *Treatise on Geophysics, Volume 3 Geodesy*, 2009.

S. Englich, R. Heinkelmann, and H. Schuh. Re-assessment of ocean tidal terms in high-frequency Earth rotation variations observed by VLBI. in A. Finkelstein and D. Behrend, eds. *Measuring the future. Proceedings of the 5th IVS general meeting*, (ISBN 978-5-02-025332-2):314–318, 2008.

Rüdiger Haas, Gunnar Elgered, Johan Löfgren, Tong Ning, and Hans-Georg Scherneck. Onsala Space Observatory – IVS Network Station. *IVS 2012 Annual Report*, pages 130–133, 2012.

Robert Heinkelmann. VLBI Geodesy: Observations, Analysis and Results. *Geodetic Sciences - Observations, Modeling and Applications*, (ISBN 10.5772/54446), 2013. doi: 10.5772/54446. URL http://cdn.intechopen.com/pdfs-wm/44209.pdf.

T.A. Herring. Modeling atmospheric delays in the analysis of space geodetic data. In D.. Spoelstra, ed. Netherlands Geodetic Commission, publications on Geodesy no. 36. *Refraction of Transatmospheric Signals in Geodesy*, page 157–164, 1992.

T.A. Herring, J.L. Davis, and I.I. Shapiro. Geodesy by radio interferometry: The application of kalman filtering to the analysis of very long baseline interferometry data. *J. Geophys. Res.*, 95:12561–12581, 1990.

T. Hobiger, R. Ichikawa, Y. Koyama, and T. Kondo. Fast and accurate ray-tracing algorithms for real-time space geodetic applications using numerical weather models. *J. Geoph. Res.*, 113, 2008. doi: 10.1029/2008JD010503.

D.S. MacMillan and C. Ma. Evaluation of very long baseline interferometry atmospheric modeling improvements. *J. Geophys. Res.*, 99:637–651, 1994.

Matthias Madzak, Sigrid Böhm, Hana Krasna, and Lucia Plank. *Vienna VLBI Software Version 2.1 User Manual*. Vienna University of Technology, Department of Geodesy and Geoinformation, 2013.

T. Nilsson and R. Haas. Impact of atmospheric turbulence on geodetic very long baseline interferometry. *J. Geophys. Res*, 115, B03407, 2010. doi: 10.1029/2009JB006579.

A. Pany, J. Böhm, D. MacMillan, H. Schuh, T. Nilsson, and J. Wresnik. Monte Carlo simulations of the impact of troposphere, clock and measurement errors on the repeatability of VLBI positions. *J. Geod.*, 85:39–50, 2010. doi: 10.1007/s00190-010-0415-1.

G. Petit and eds. Luzum, B. IERS Conventions 2010. Frankfurt am Main: Verlag des Bundesamts für Kartographie und Geodäsie, IERS Technical Note No. 36. 2010.

Bill Petrachenko, Arthur Niell, Dirk Behrend, Brian Corey, Johannes Böhm, Patrick Charlot, Arnaud Collioud, John Gipson, Yasuhiro Koyama Dan MacMillan Zinovy Malkin Rüdiger Haas, Thomas Hobiger, Tobias Nilsson, Andrea Pany, Gino Tuccari, Alan Whitney, and Jörg Wresnik. Design Aspects of the VLBI2010 System. *Progress Report of the IVS VLBI2010 Committee*, 2009.

L. Petrov and J.P. Boy. Study of the atmospheric pressure loading signal in very long baseline interferometry observations. *J. Geophys. Res.*, 109, 2004.

L. Petrov, D. Gordon, J. Gipson, D. MacMillan, C. Ma, E. Fomalont, R.C. Walker, and C. Carabajal. Precise geodesy with the Very Long Baseline Array. *J. Geod.*, 83:859–876, 2009.

Carsten Rieck, Rüdiger Haas, Per Jarlemark, and Kenneth Jaldehag. VLBI Frequency Transfer using CONT11. *Proceedings of European Frequency and Time Forum (EFTF)*, 2012. doi: 10.1109/EFTF.2012.6502358.

Westford MA Rogers, A.E.E. Haystack Observatory. A receiver phase and group delay calibrator for use in very long baseline interferometry. *Haystack Observatory Technical Note*, 1975.

H.G. Scherneck. A parameterized solid earth tide model and ocean tide loading effects for global geodetic baseline measurements. *Geophys. J. Int.*, 106:677–694, 1991.

Caroline Schönberger, Paul Gnilsen, Johannes Böhm, and Rüdiger Haas. Twin Telescopes at Onsala and Wettzell and their contribution to the Very Long Baseline Interferometry Global Observing System. Technical report, 2015. URL `http://publications.lib.chalmers.se/records/fulltext/226075/local_226075.pdf`.

H. Schuh. Die Radiointerferometrie auf langen Basen zur Bestimmung von Punktverschiebungen und Erdrotationsparametern. *DGK Reihe C, Dissertationen*, Heft Nr. 328.

H. Schuh and D. Behrend. Institute of Geodesy and Geophysics, University of Technology, Vienna, Austria, VLBI: A fascinating technique for Geodesy and Astrometry. *Journal of Geodynamics 61*, pages 68–80, 2012. URL `http://dx.doi.org/10.1016/j.jog.2012.07.007`.

H. Schuh and L. Plank. Radiointerferometrie auf langen Basen (VLBI - Very Long Baseline Interferometry), lecture notes. 2011.

Harald Schuh. Introduction to Advanced Geodesy, lecture notes. 2011.

Harald Schuh and Johannes Böhm. Very Long Baseline Interferometry for Geodesy and Astrometry, in Guochang Xu, Sciences of Geodesy II, Innovations and Future Developments. (ISBN 978-3-642-27999-7):339–376, 2013. doi: 10.1007/978-3-642-28000-9.

Harld Schuh, Johannes Böhm, Sigrid Böhm, Nafisi Vahab, Tobias Nilsson, Andrea Pany, Lucia Plank, Hana Krasna, Jing Sun, and Kamil Teke. *The Vienna VLBI Software Version 1c.* Manual. Vienna University of Technology Department of Geodesy and Geoinformation, 2010.

O.J. Sovers, J.L. Fanselow, and C.S. Jacobs. Astrometry and geodesy with radio interferometry: experiments, models, results. *Reviews of Modern Physics*, 70:1393–1454, 1998.

Jing Sun, Tobias Nilsson, Johannes Böhm, and Harald Schuh. Institute of Geodesy and Geophysics, Vienna University of Technology. new Observing Strategies with Twin Telescopes for Geodetic VLBI. *IVS 2012 General Meeting Proceedings*, pages 28–32, 2012. URL `http://ivscc.gsfc.nasa.gov/publications/gm2012/sun.pdf`.

Jing Sun, Johannes Böhm, Tobias Nilsson, Hana Krásná, Sigrid Böhm, and Harald Schuh. New VLBI2010 scheduling strategies and implications on the terrestrial reference frames, Institute of Geodesy and Geophysics, Vienna University of Technology. *J Geod*, 88: 449–461, 2014. doi: 10.1007/s00190-014-0697-9.

F. Takahashi, T. Kondo, Y. Takahashi, and Y. Koyama. Wave Summit Course: Very Long Baseline Interferometer. *IOS Press*, (ISBN 1-58603-076-0), 2000.

K. Teke, R. Heinkelmann, J. Böhm, and H. Schuh. VLBI Baseline Length Repeatability Tests of IVS-R1 and -R4 Session Types. in A. Finkelstein and D. Behrend, eds. *'Measuring the Future', Proceedings of the 5th IVS General Meeting*, (ISBN 978-5-02-025332-2): 173–177, 2008.